Membranes

18.354 - L11

dunkel@mit.edu

Cell membranes (D=2)

transport:
stochastic
escape problems

Illustration by J.P. Cartailler. Copyright 2007, Symmation LLC.

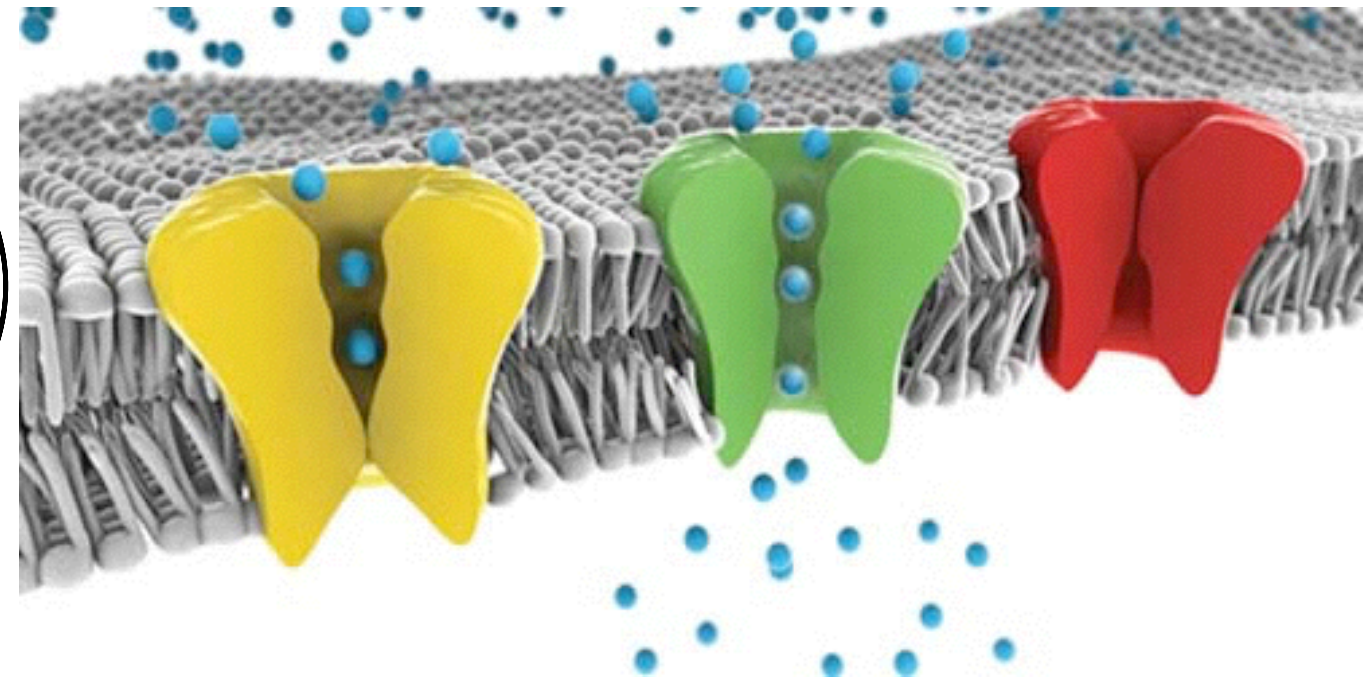

shape:
differential
geometry

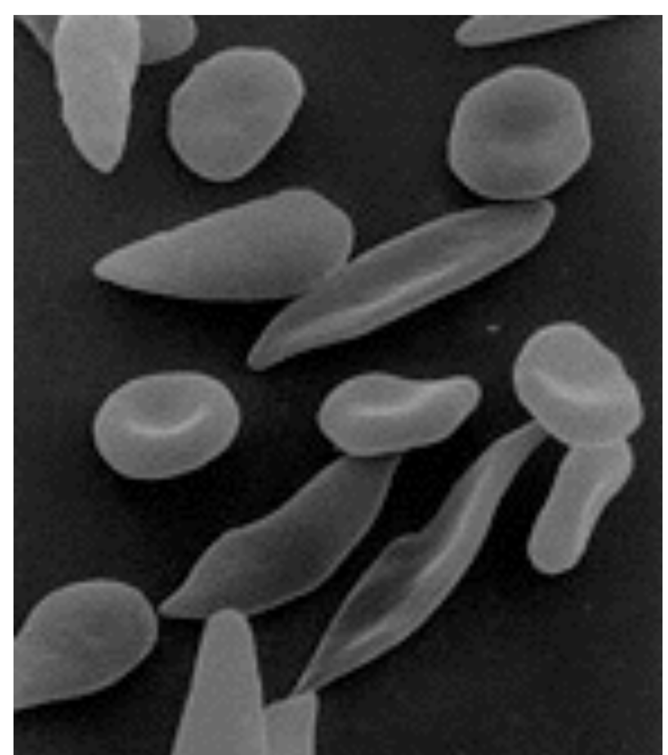

red blood cells
affected by
sickle-cell disease

source: wiki

dunkel@math.mit.edu

Cell membranes

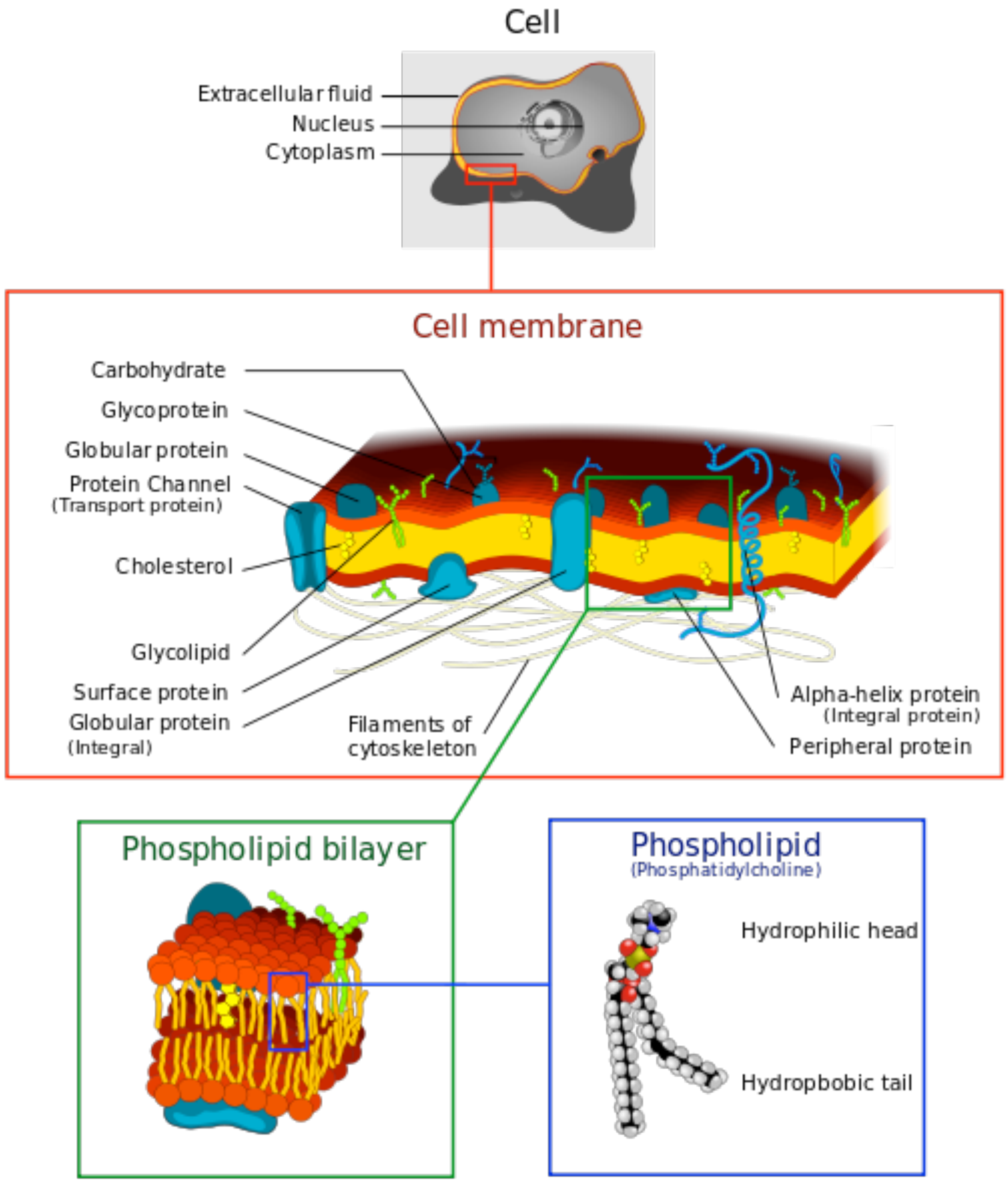

source: wiki

dunkel@math.mit.edu

AFM

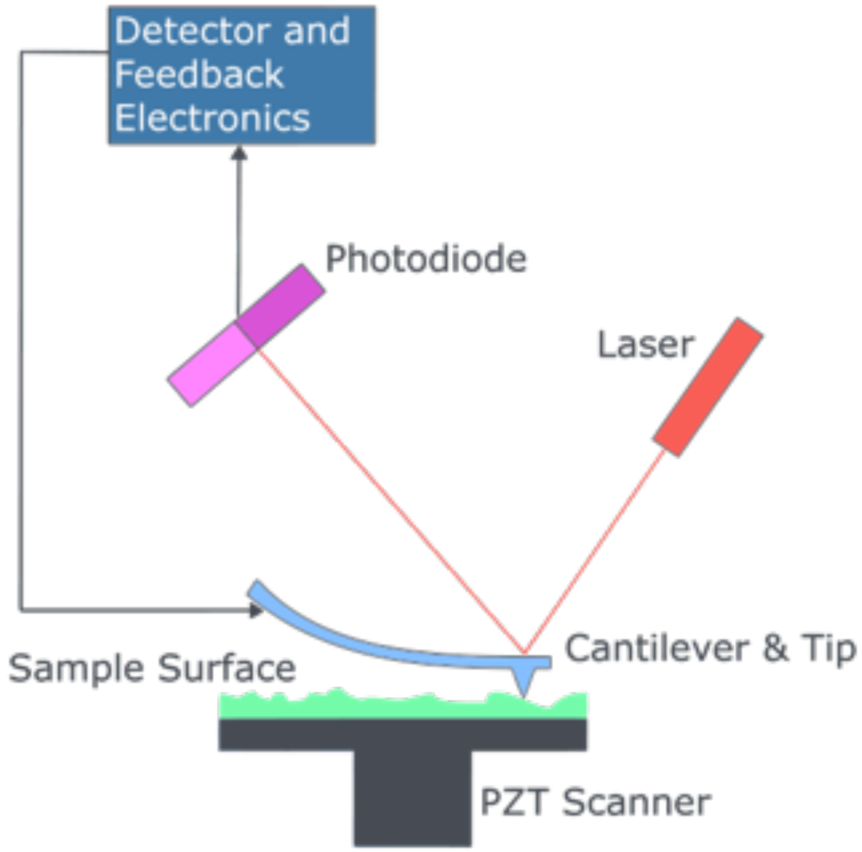

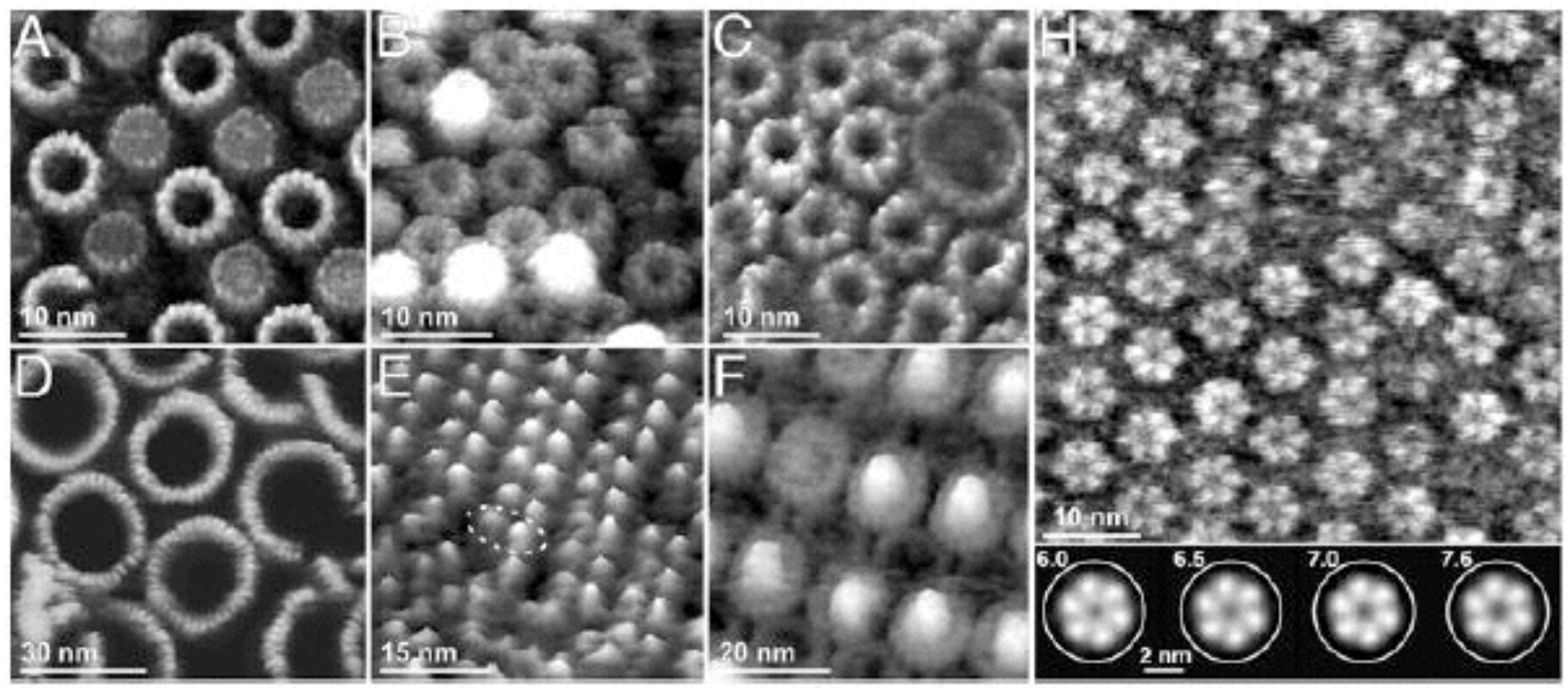

http://www.sbmp-itn.eu/sbmps/research_method/

source: wiki

dunkel@math.mit.edu

Bio-membrane

Selective barrier

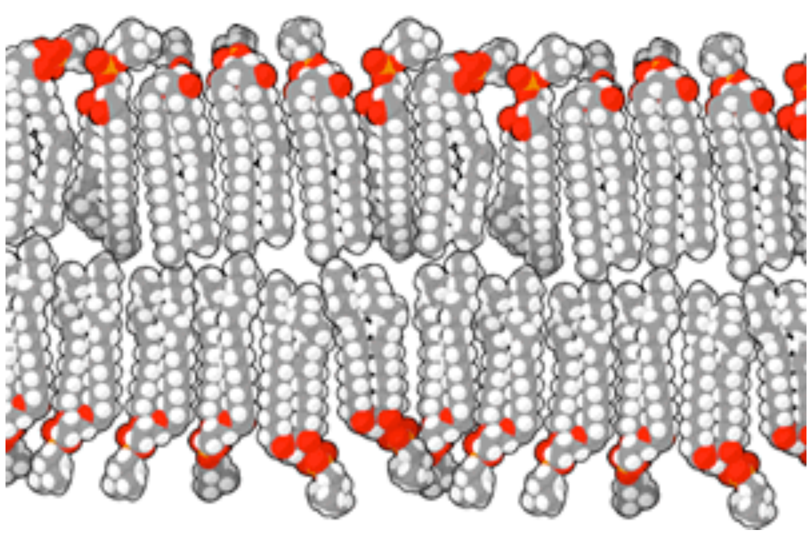

source: wiki

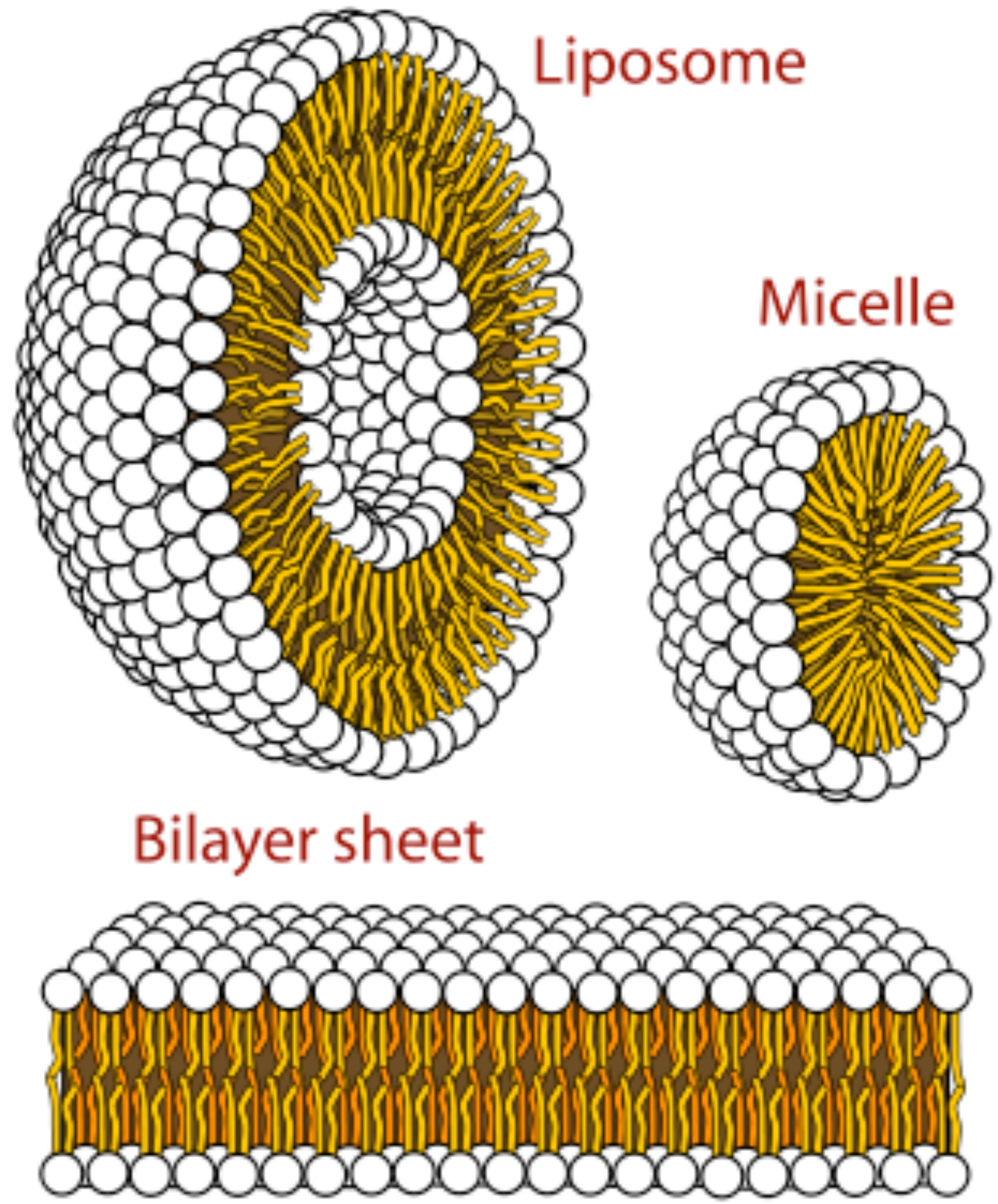

dunkel@math.mit.edu

Morphological changes

e.g., fusion through stalk-formation

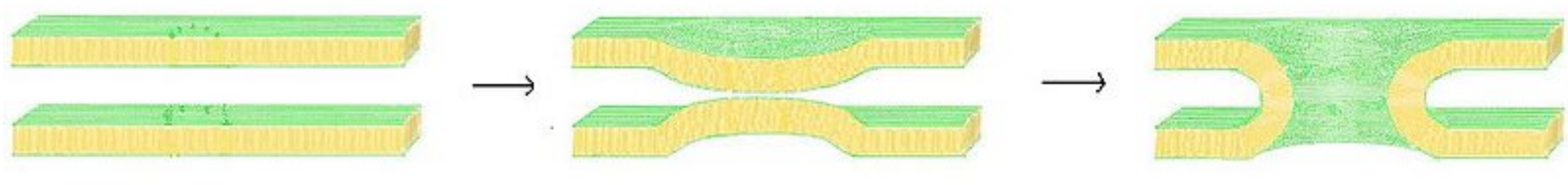

source: wiki

dunkel@math.mit.edu

Endo- & Exocytosis

material exchange with environment

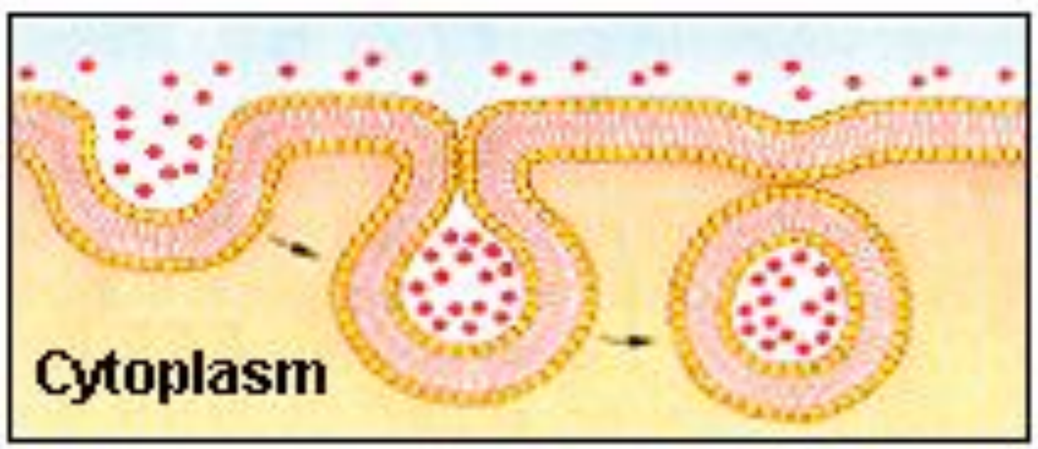

Endocytosis

A bit of plasma membrane baloons inwai
beneath water and solutes outside, then
pinches off as an endocytic vesicle that
moves into the cytoplasm

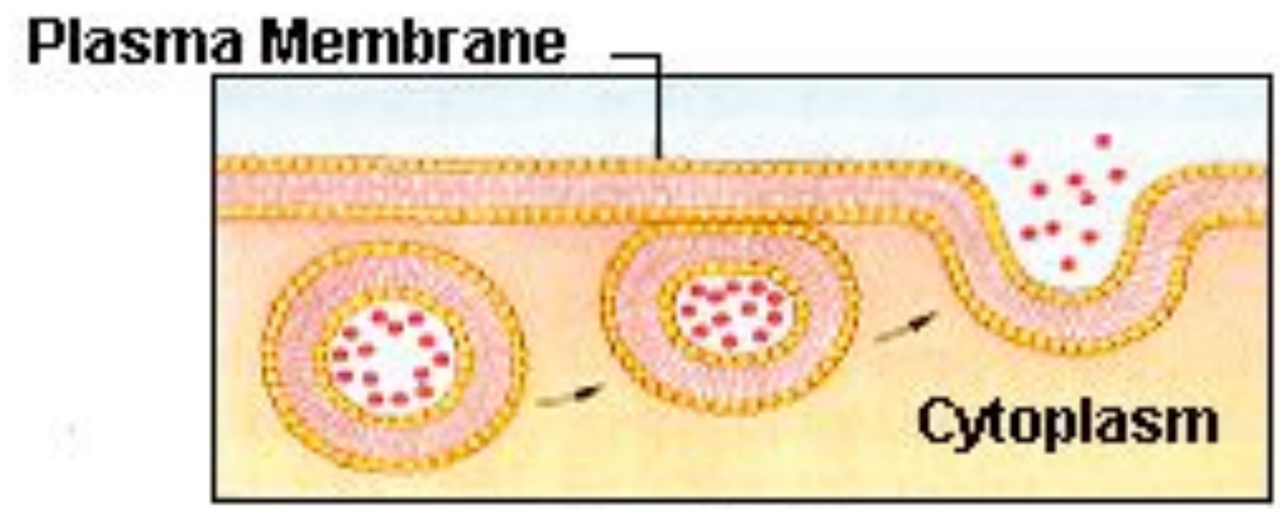

Exocytosis

Cells release substances when an
exocytic vesicle's membrane fuses
with the plasma membrane

dunkel@math.mit.edu

Active transport

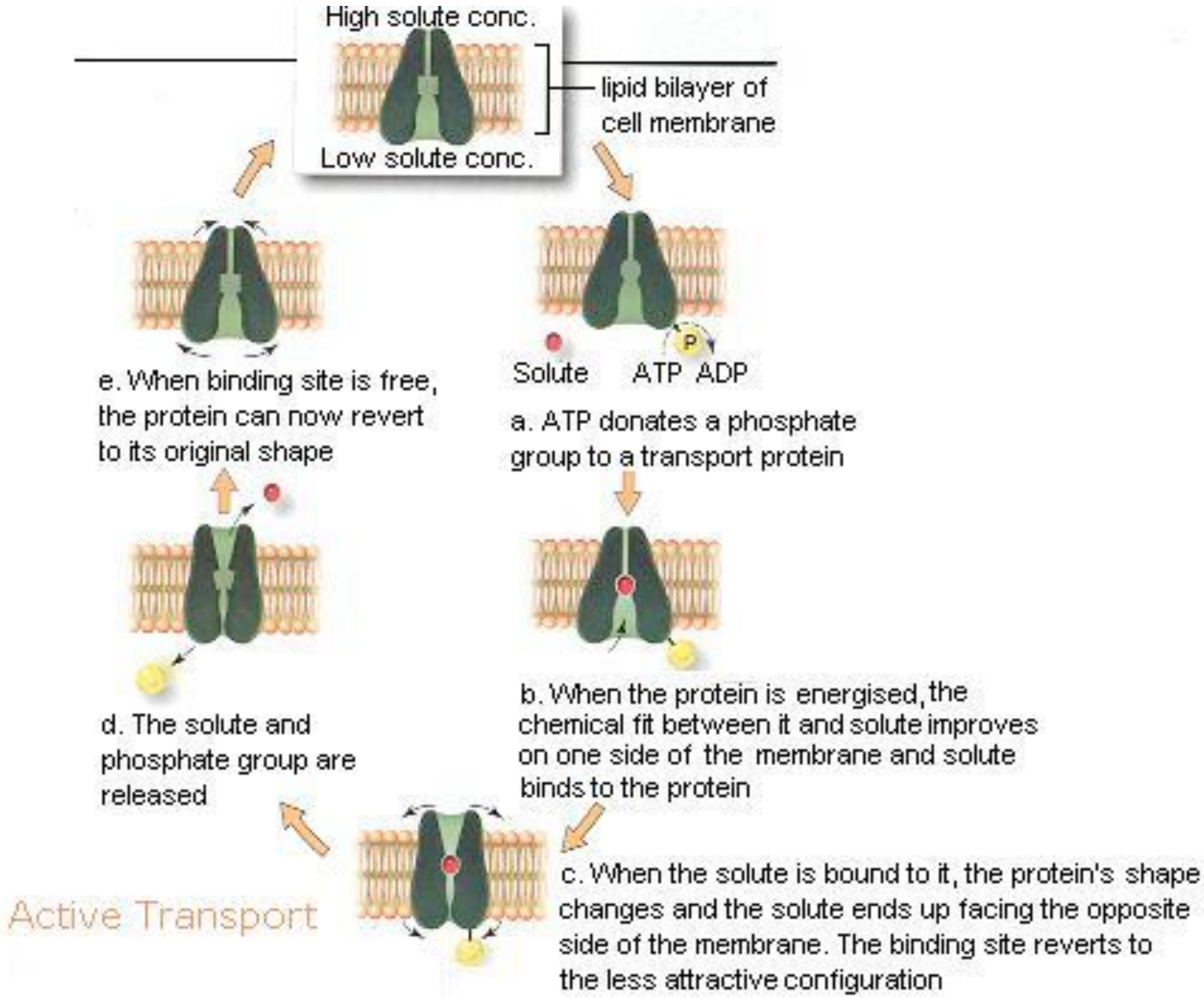

Intercellular gap junctions

exchange of molecules and ions between animal cells

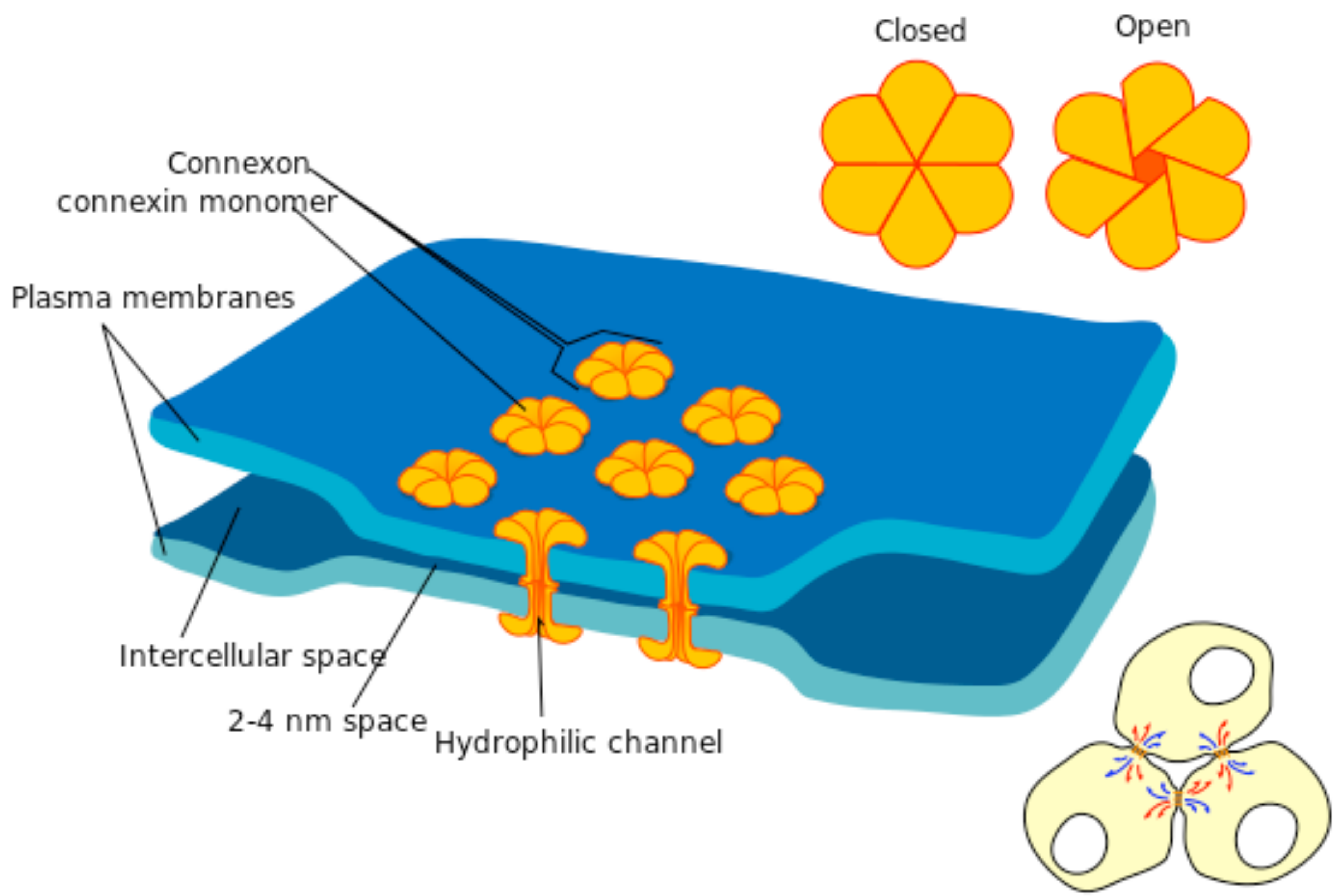

source: wiki

dunkel@math.mit.edu

Virus envelop

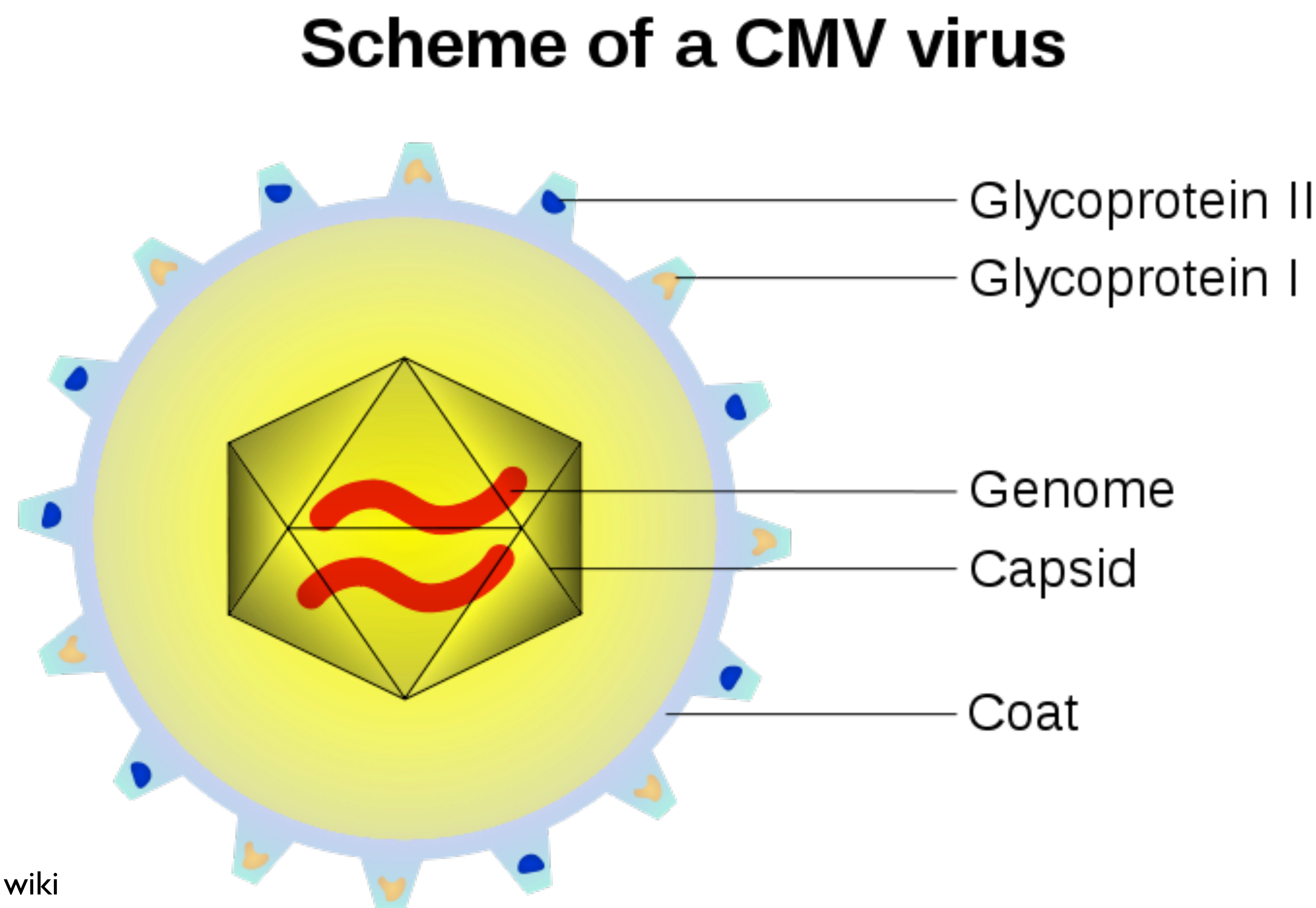

source: wiki

envelop fuses with host membrane

Capsid

cryo-EM

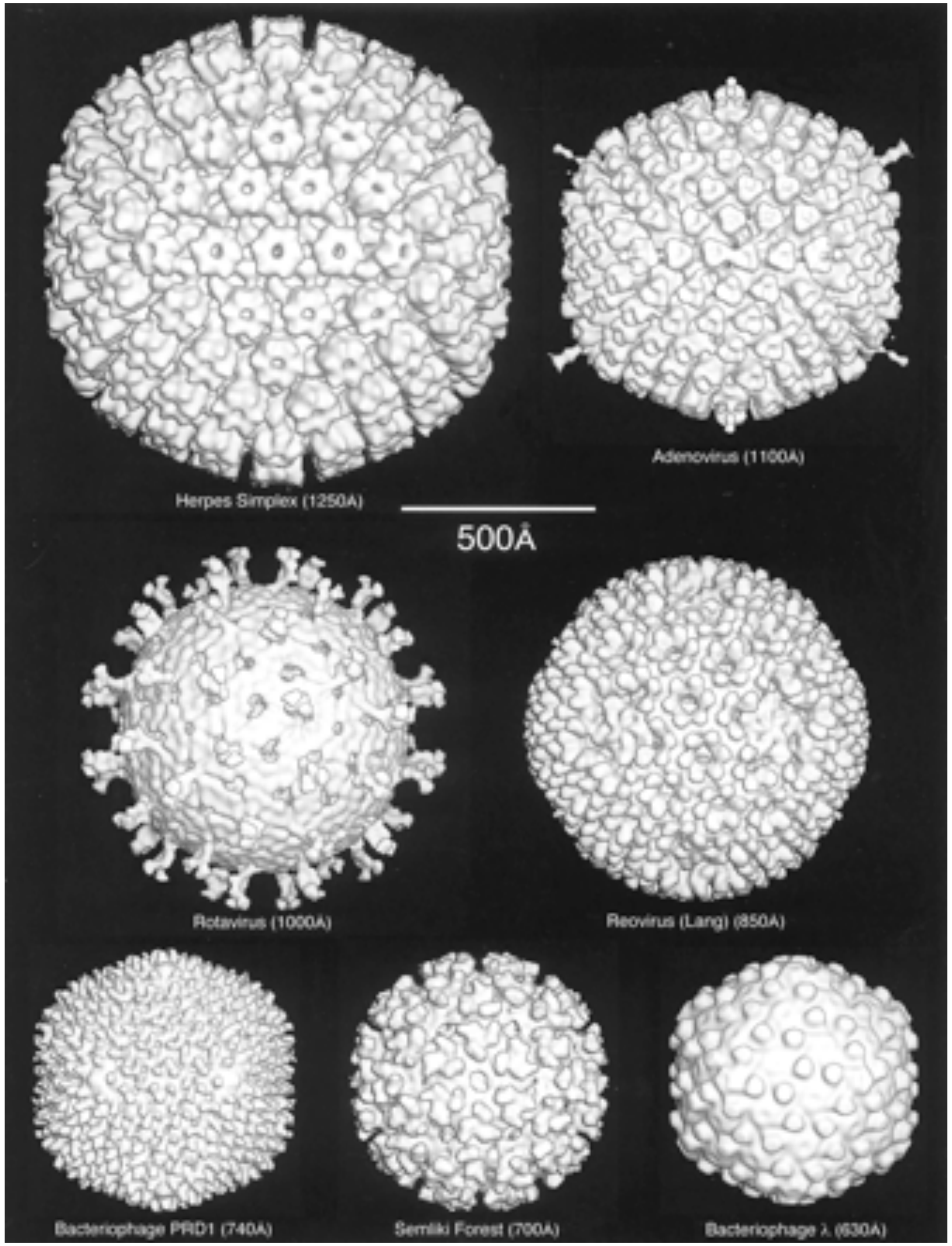

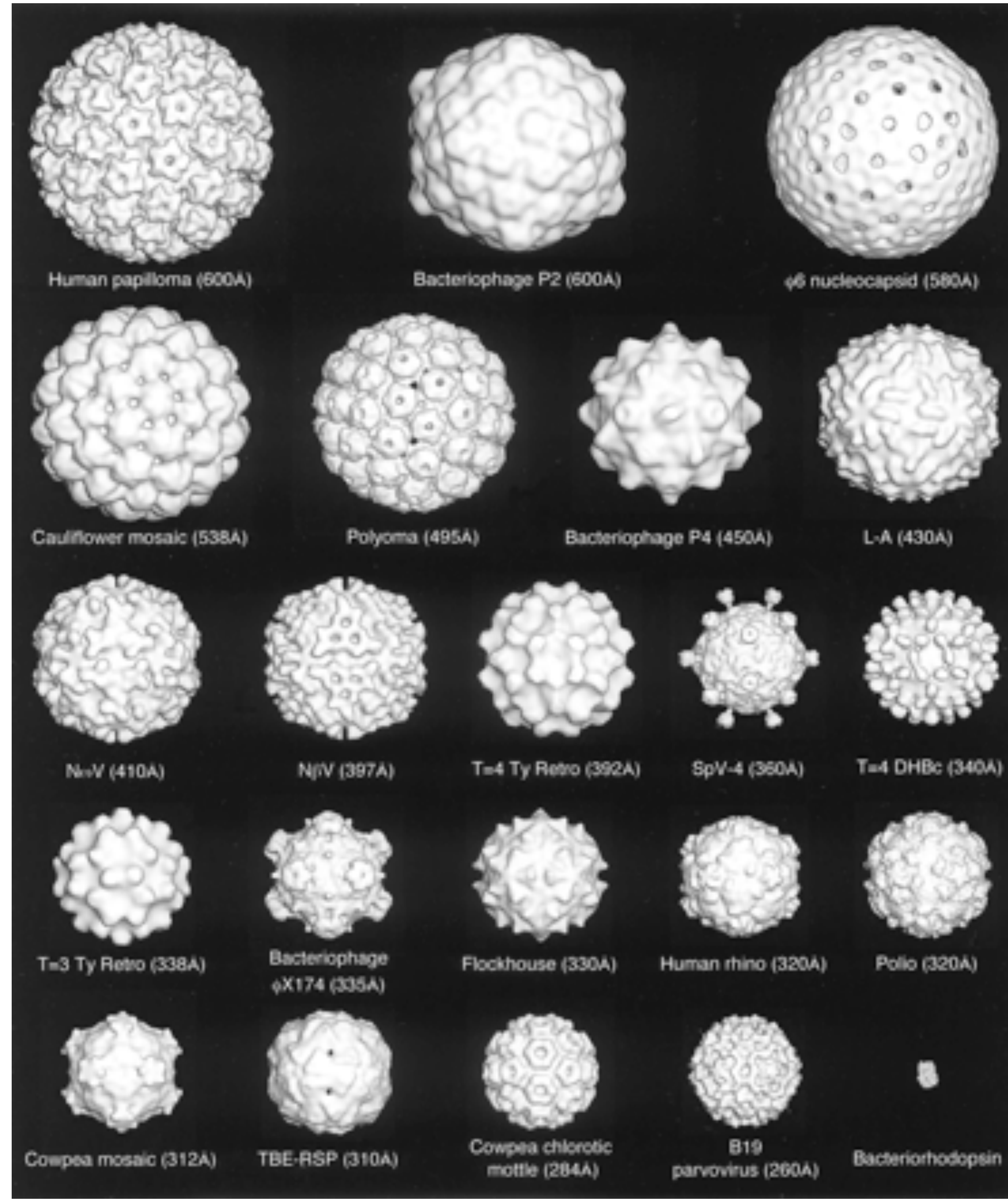

Baker et al (1999) MMBR

dunkel@math.mit.edu

Diatoms (algae)

H_4SiO_4

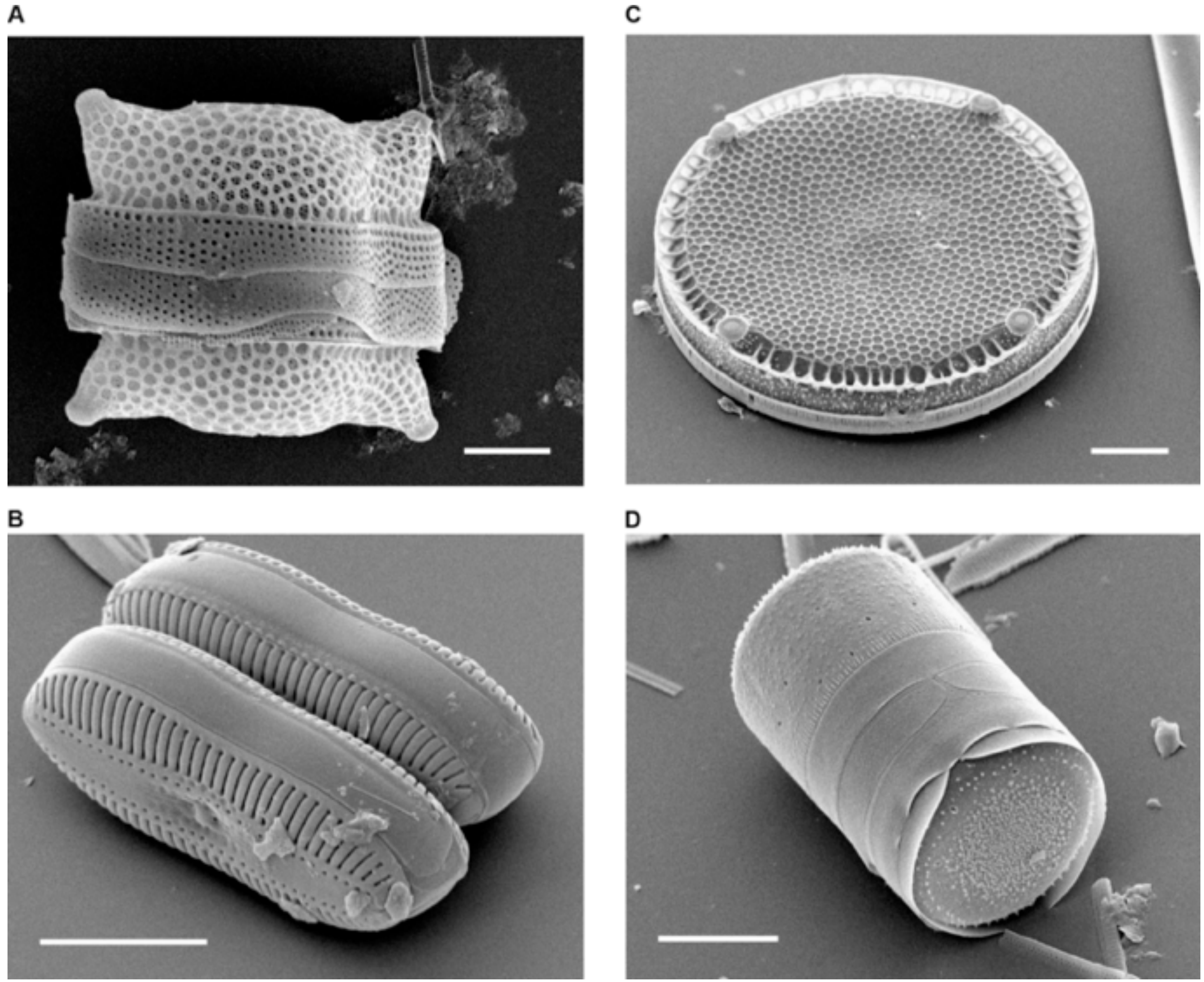

source: wiki

More planktonic diatoms

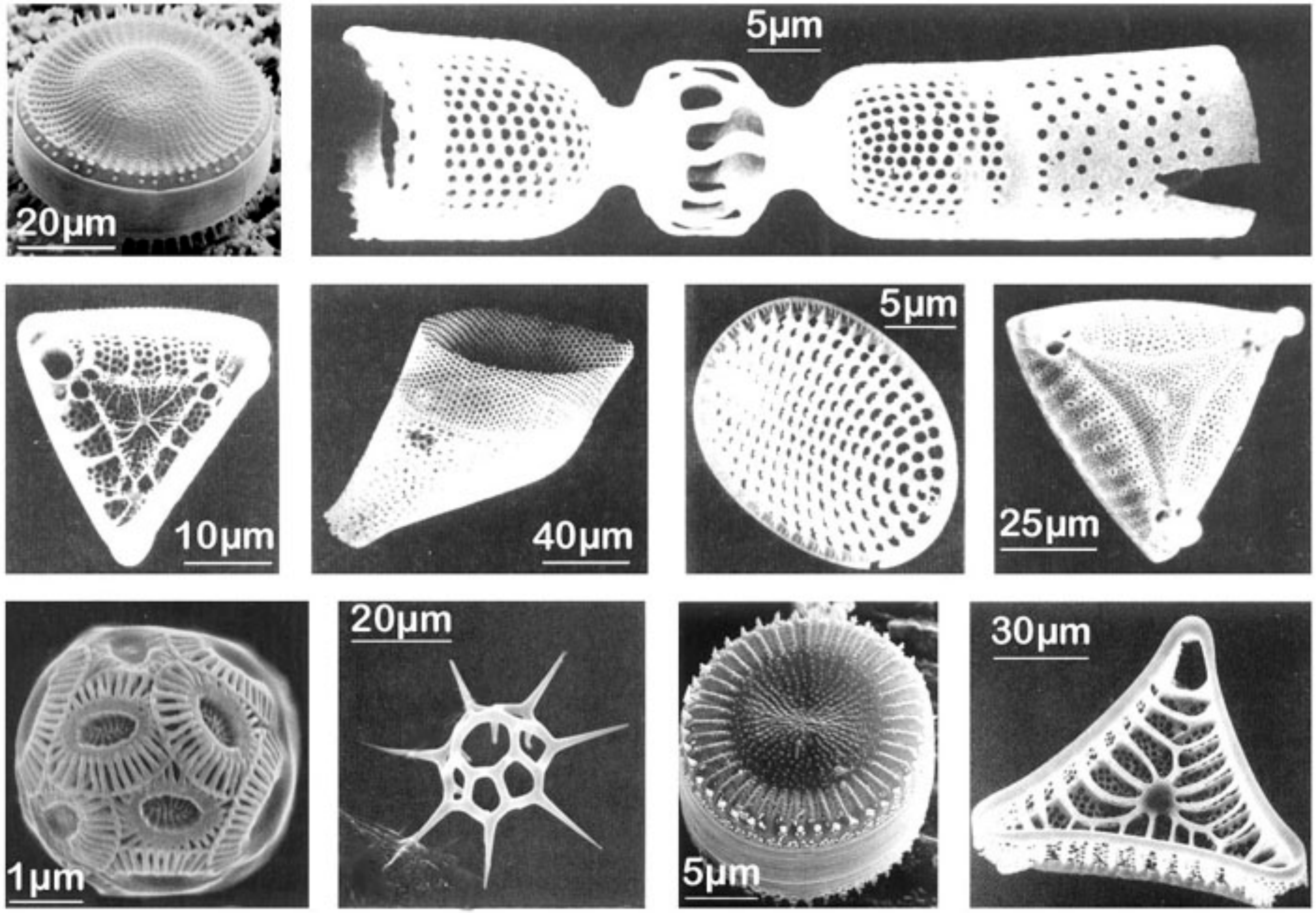

Selection of planktonic diatoms
(not representative for the mediterranian)

dunkel@math.mit.edu

Plants

unlike animal cells, every plant cell is surrounded by a polysaccharide cell wall

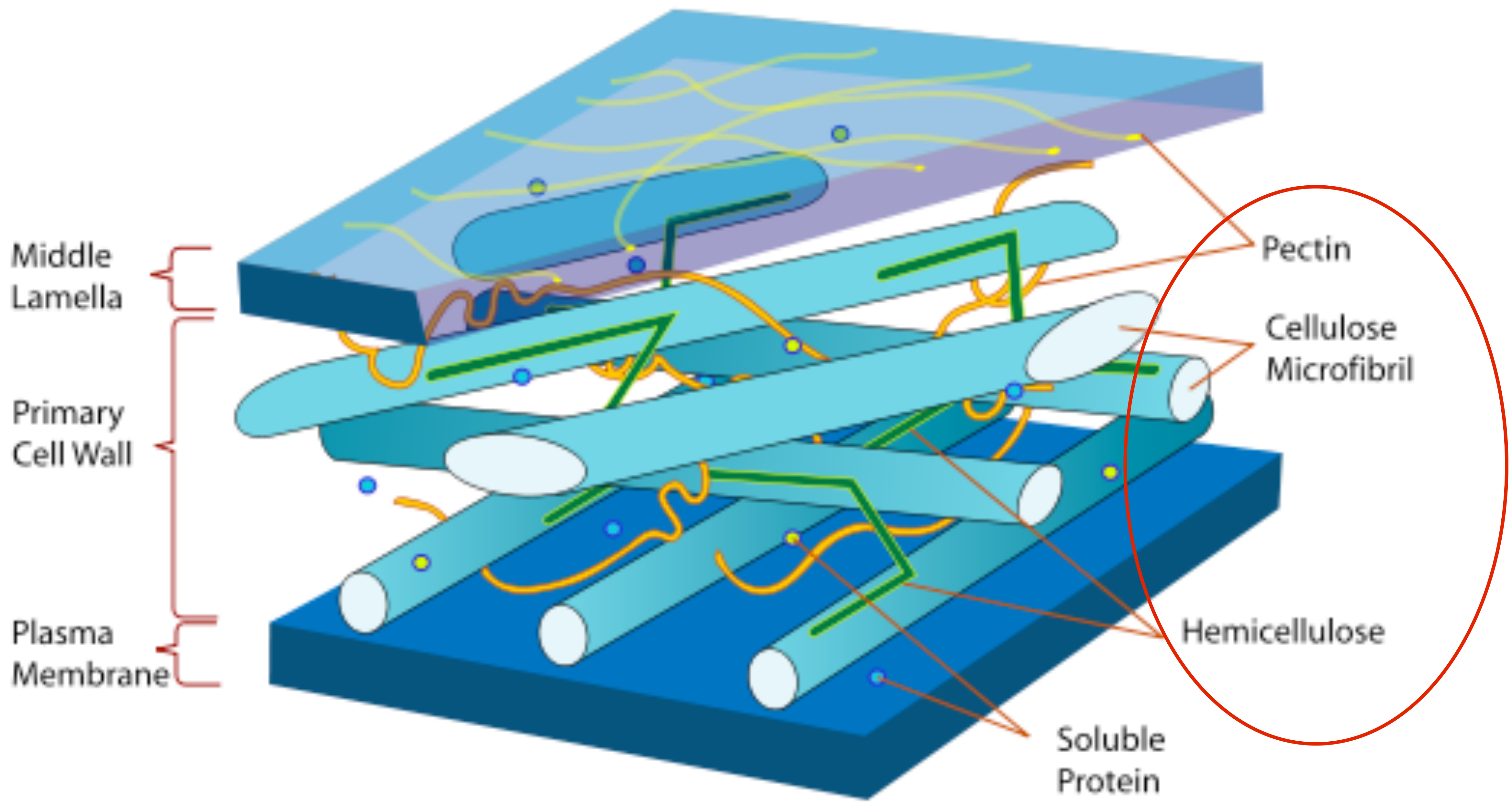

source: wiki

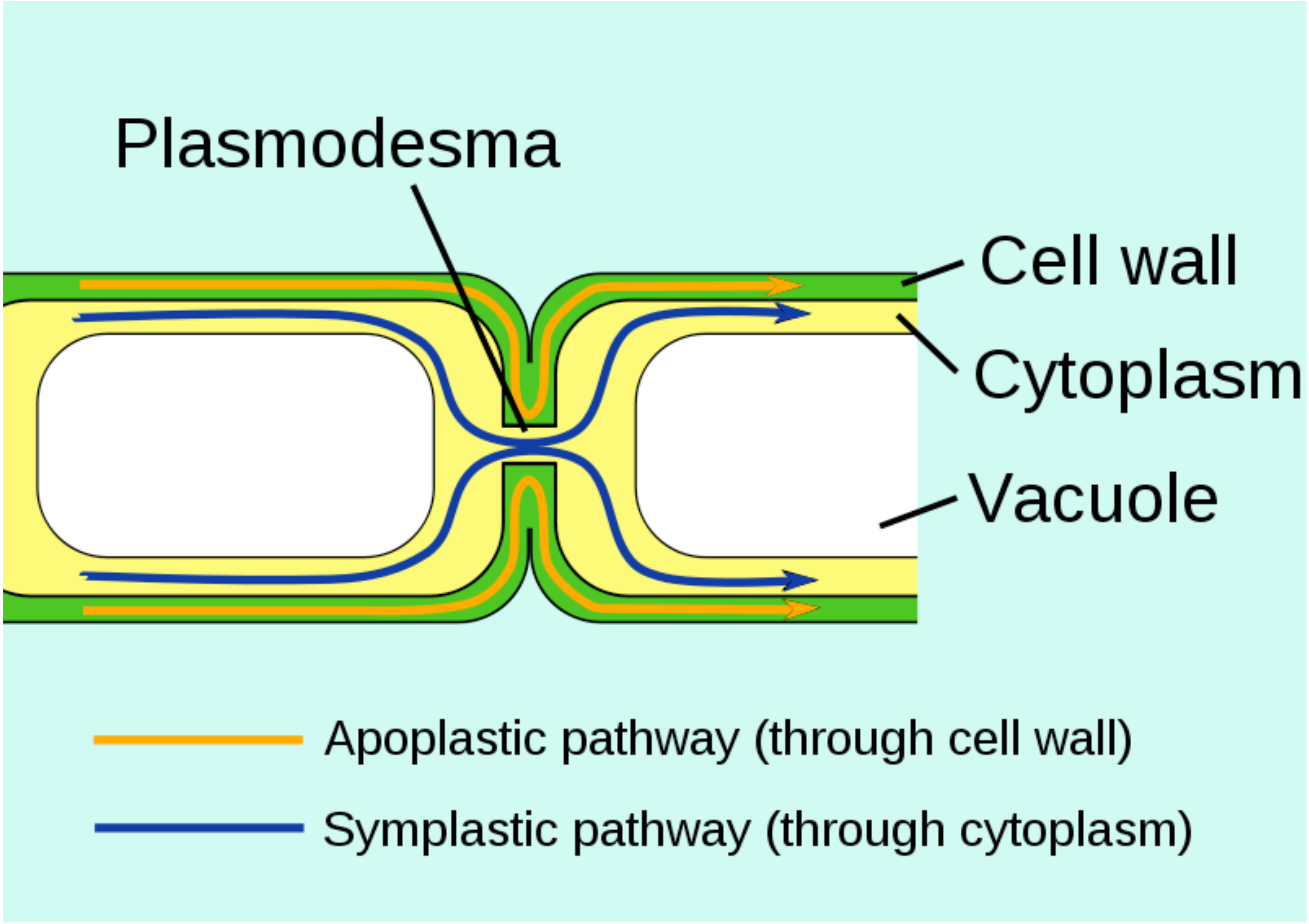

typical plant cell has between 10^3 and 10^5 plasmodesmata
connecting it with adjacent cells
equating to between 1 and 10 per μm

source: wiki

dunkel@math.mit.edu

Chara fragilis

http://www.youtube.com/watch?feature=player_detailpage&v=kud4qUhsCxg

dunkel@math.mit.edu

Characean algae

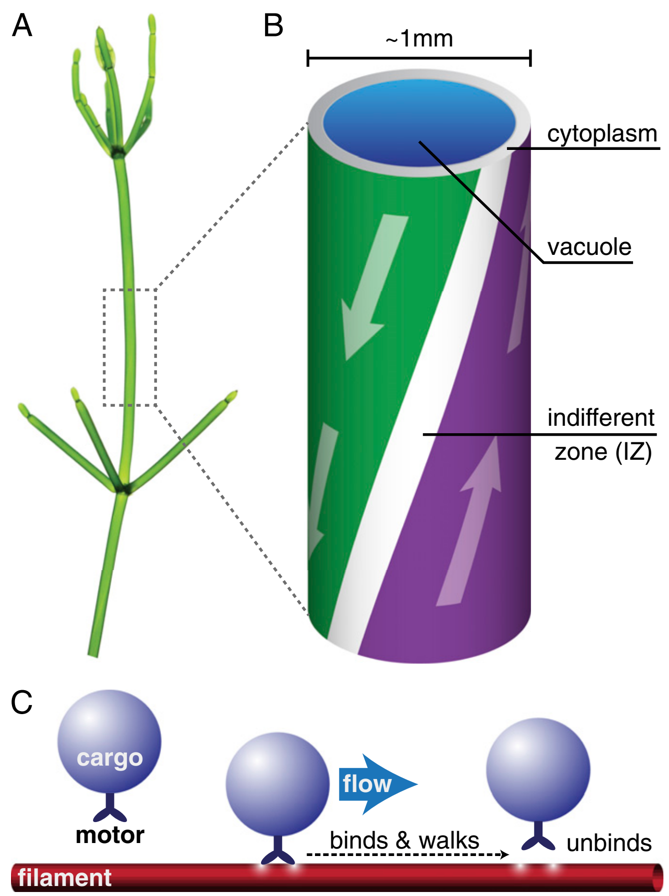

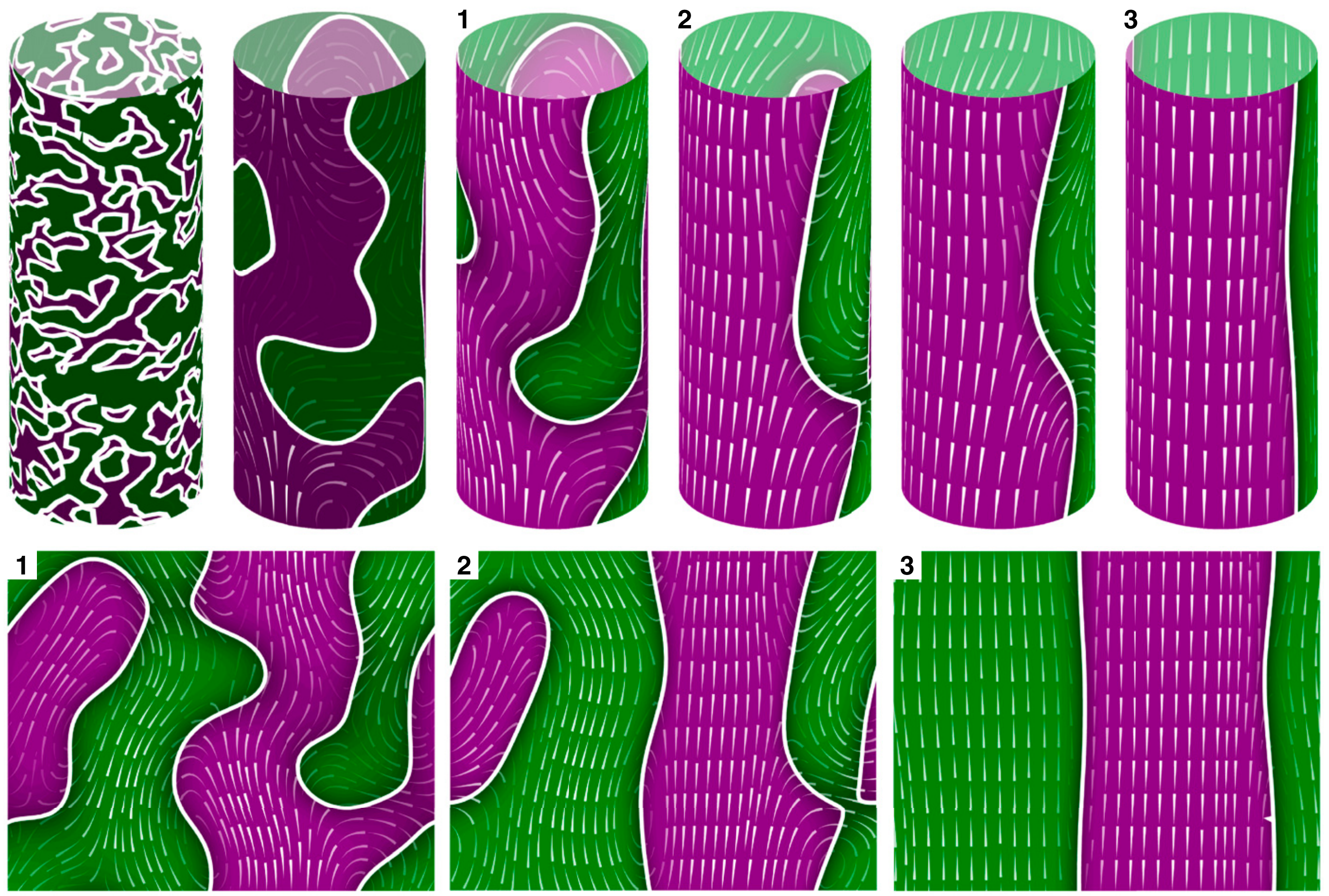

$$-\mu\nabla^2\mathbf{u}+\mathbf{u}+\Pi_0\mathbf{e}_z+\nabla\Pi'=|\mathbf{P}|^2\,\mathbf{P},$$

$$\nabla\cdot\mathbf{u}=0$$

$$\frac{\partial\mathbf{P}}{\partial t}+\epsilon\mathbf{u}\cdot\nabla\mathbf{P}=d^{(s)}\nabla^2\mathbf{P}-d^{(r)}\mathbf{P}+(\mathbb{I}-\mathbf{PP})\cdot\big[\epsilon(\nabla\mathbf{u})\cdot\mathbf{P}$$
$$+\alpha_p\mathbf{P}+\alpha_u\mathbf{u}-\kappa(\mathbf{P}\cdot\mathbf{d})\mathbf{d}\big],$$

Woodhouse & Goldstein (2013) PNAS

dunkel@math.mit.edu

Blood cells: shape & function

source: wiki

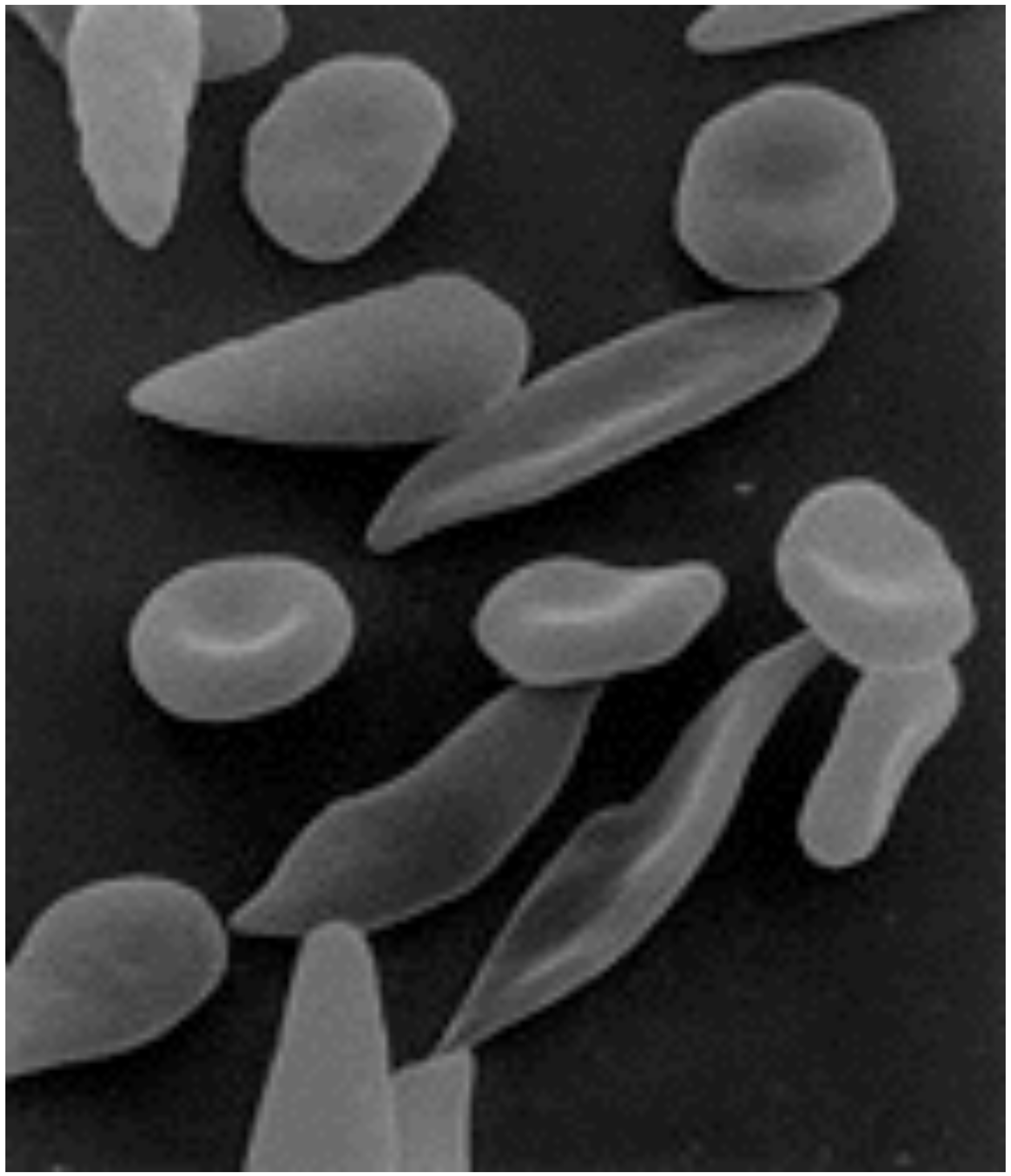

red blood cells affected by sickle-cell disease

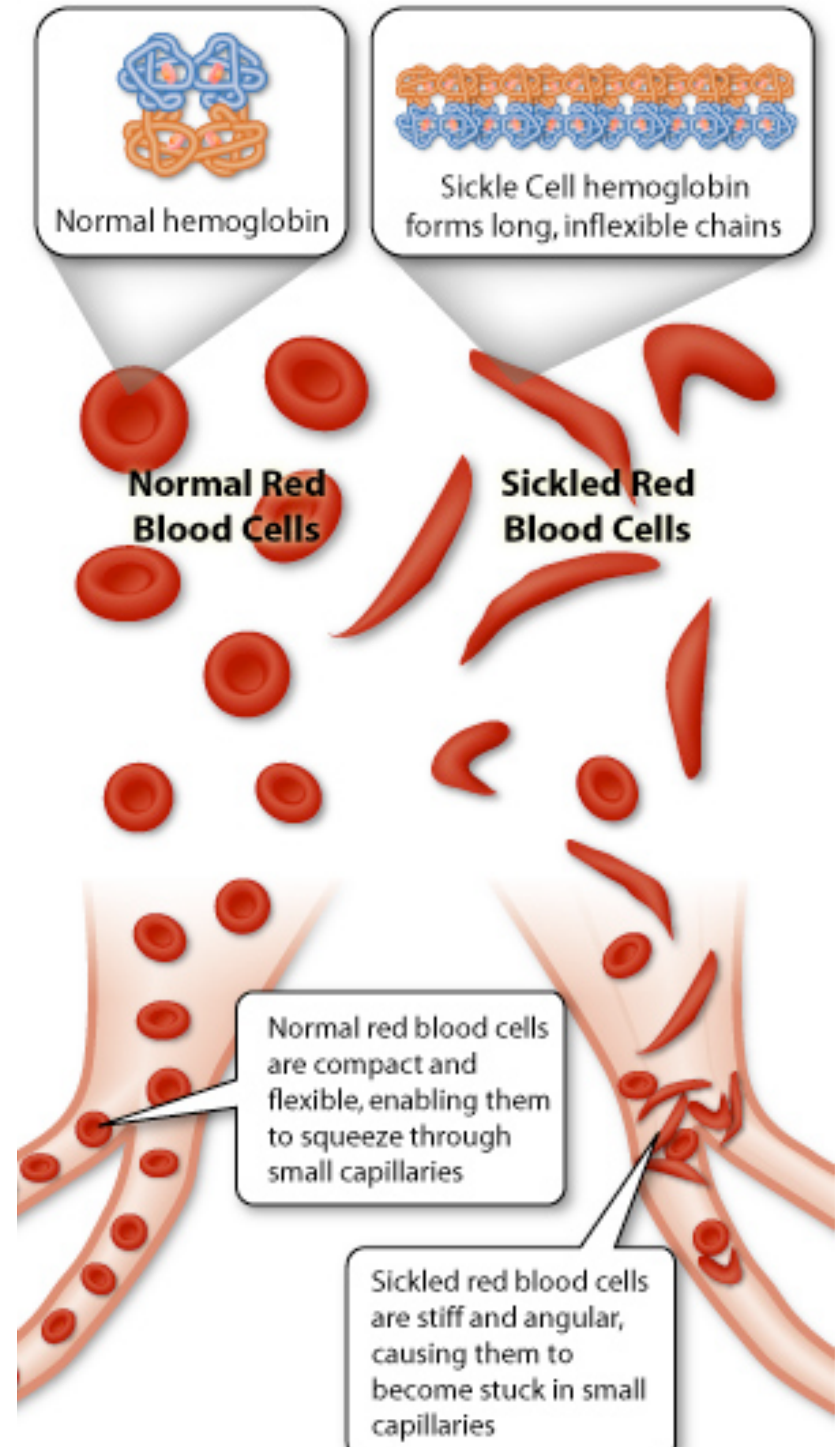

http://learn.genetics.utah.edu/

dunkel@math.mit.edu

Optical tweezer

source: wiki

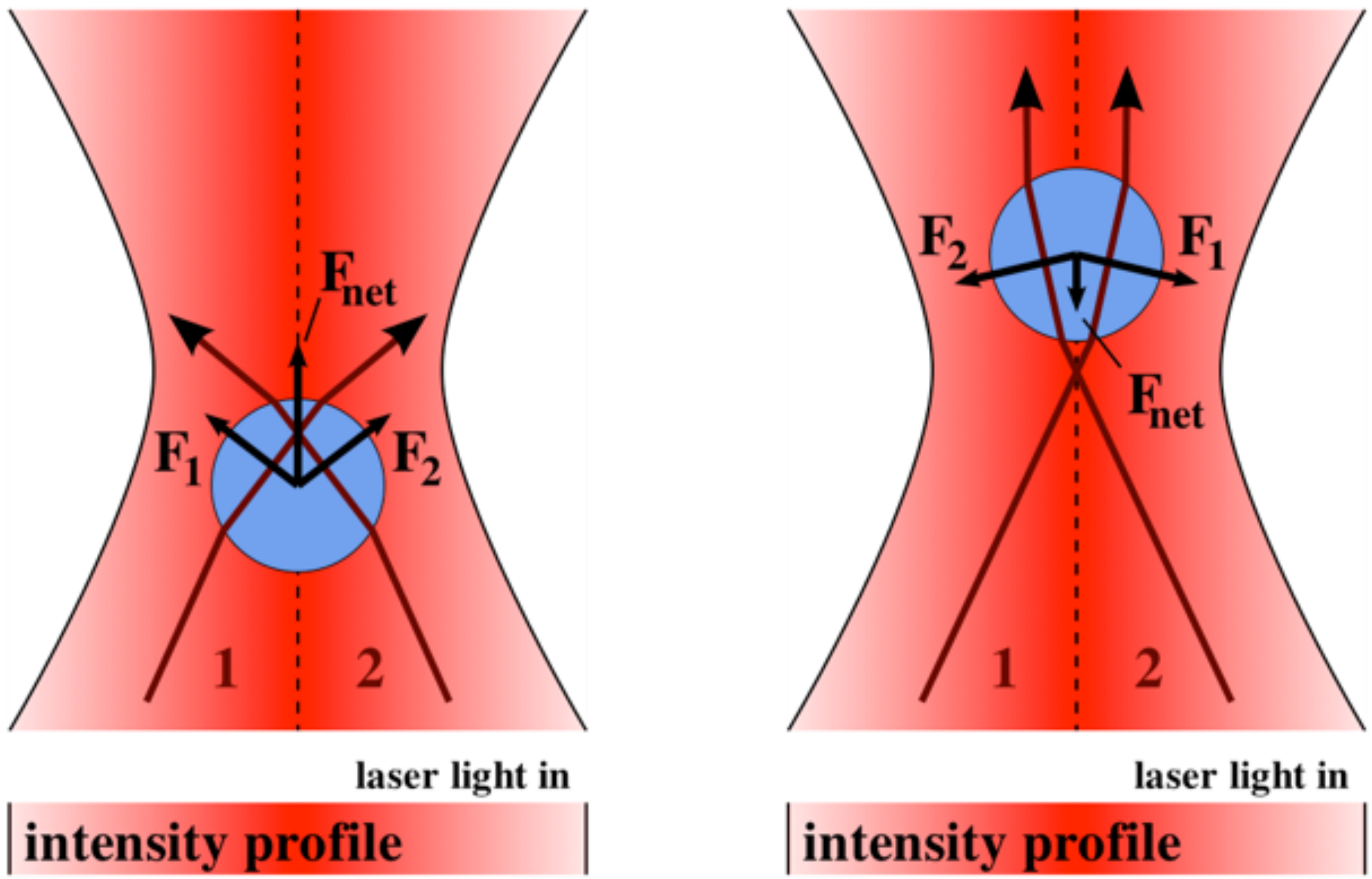

http://www.nature.com/ncomms/journal/v4/n4/extref/ncomms2786-s1.swf

dunkel@math.mit.edu

Red blood cell in tweezer

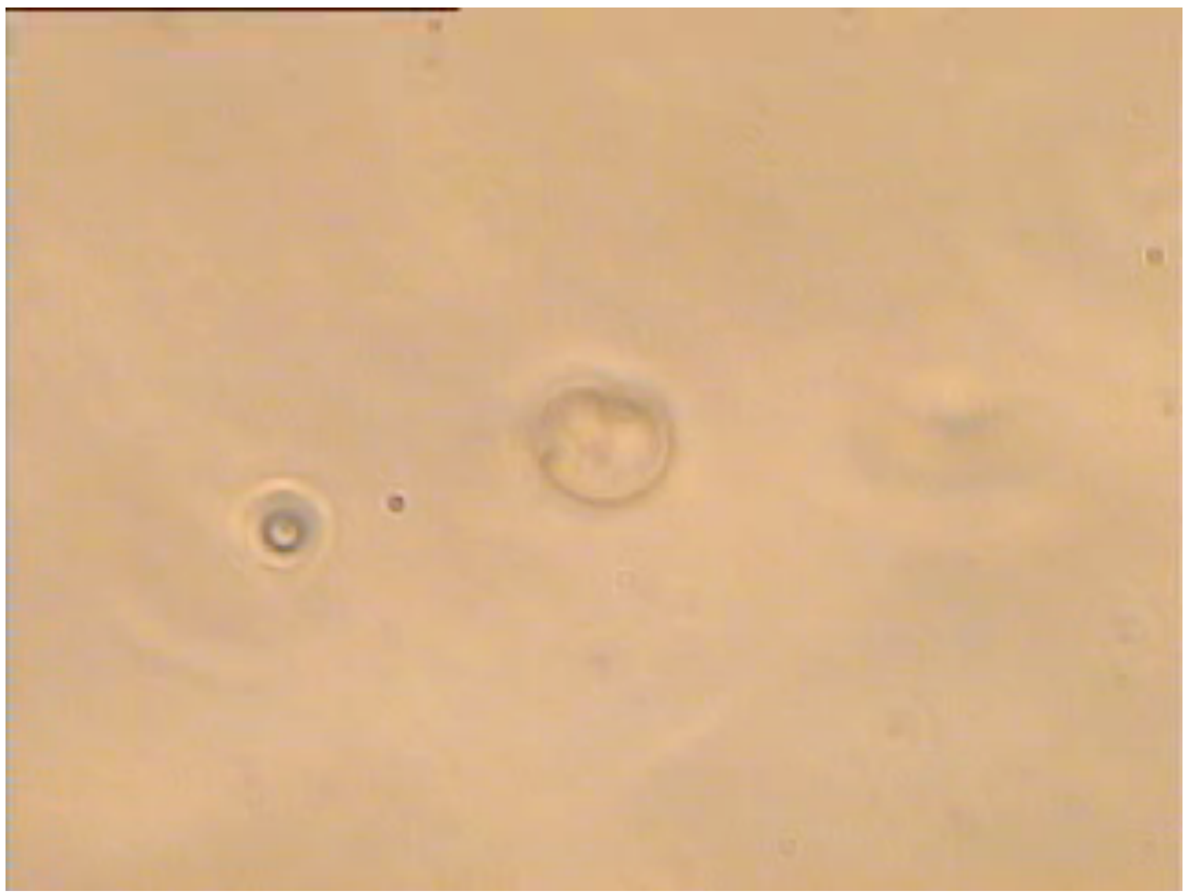

Basu et al (2011) Biophys J

dunkel@math.mit.edu

Full dynamics of a red blood cell in shear flow

Jules Dupire, Marius Socol, and Annie Viallat[1]

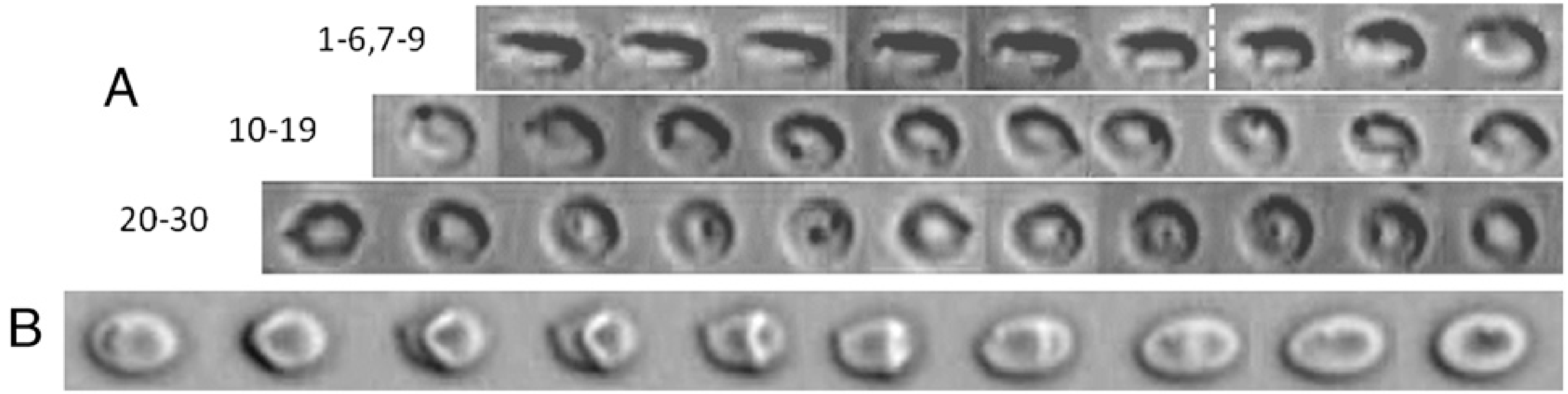

Fig. 5. Rolling-to-tank-treading transition observed on RBCs bearing a bead; dextran 2 10^6 g/mol, c = 9% (wt/wt); scale bar, 8 μm; top-view observation. (*A*) Shear rate = 3 s^{-1}. The symmetry axis of the rolling cell (images 1–7) rotates gradually (images 8–10). The spinning about the symmetry axis is detected by the bead motion (images 10–19). Finally, the streamlines change and the cell tank-treads (images 20–30). A vertical bar separates the different movements. Sequence of 46.6 s; scale bar, 7 μm. (*B*) The tank-treading movement at the transition sometimes presents an overall rotation of part of the membrane, which behaves locally like a solid by rotating as a whole. $\dot{\gamma} = 6\ s^{-1}$, time sequence of 1.98 s.

PNAS 2012

PNAS

Full dynamics of a red blood cell in shear flow

Jules Dupire, Marius Socol, and Annie Viallat[1]

Blood cell - simulations

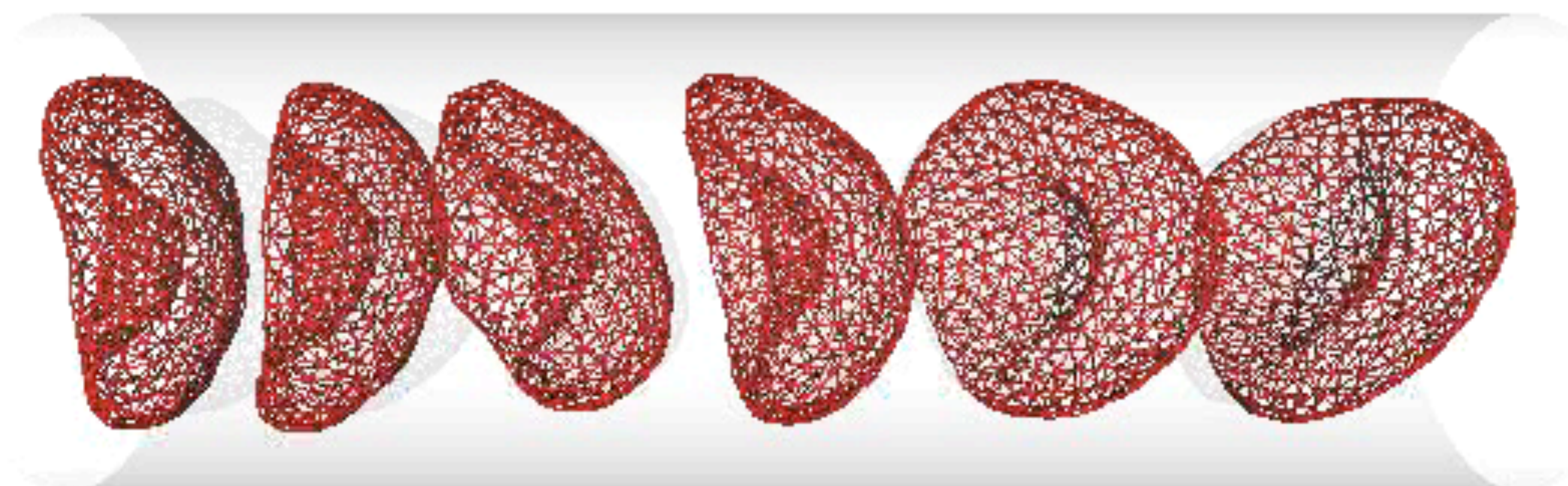

McWhirter et al (2012) New J Phys

Vesicles ("artificial" cells)

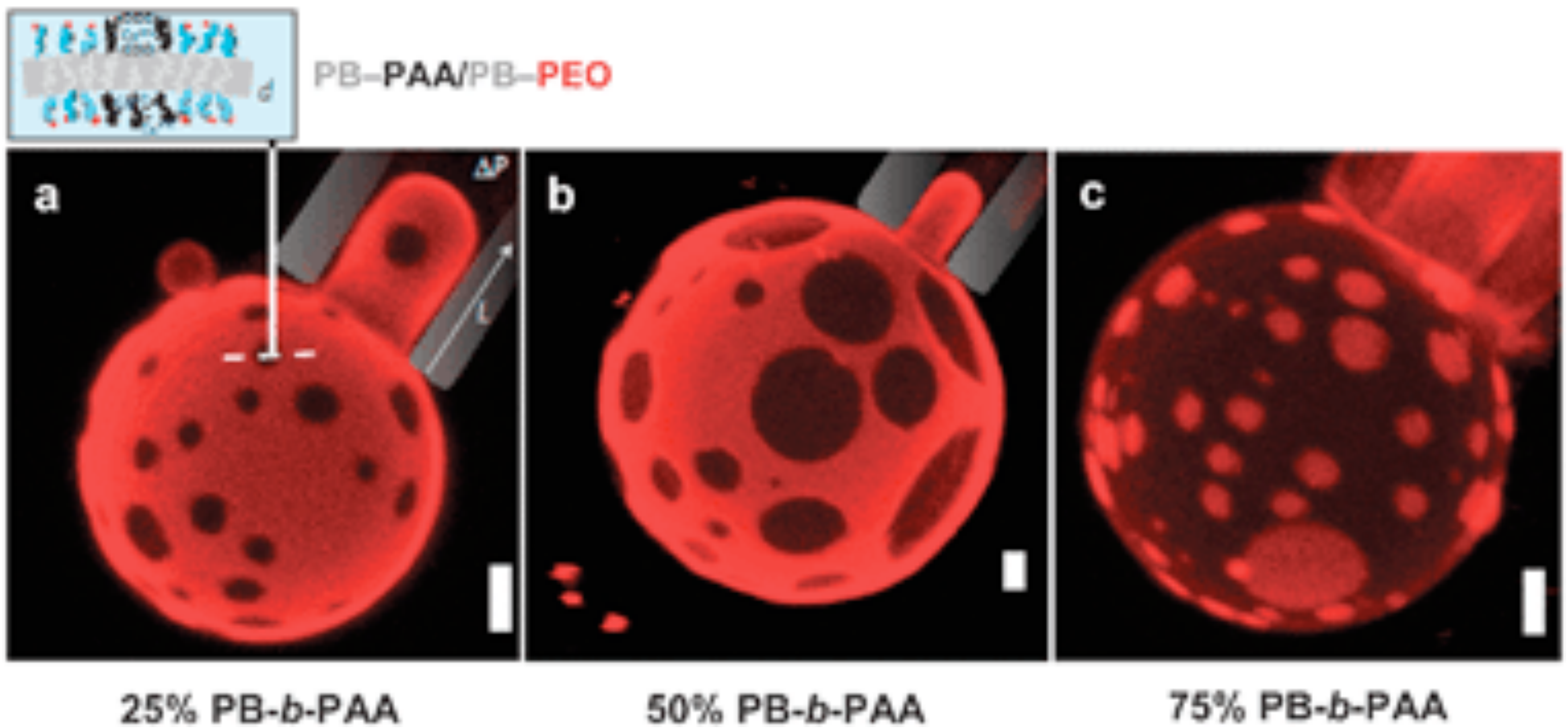

Mai & Eisenberg
Chem Soc Rev 2012

Membrane Viscosity Determined from Shear-Driven Flow in Giant Vesicles

Aurelia R. Honerkamp-Smith, Francis G. Woodhouse, Vasily Kantsler, and Raymond E. Goldstein
Department of Applied Mathematics and Theoretical Physics, Centre for Mathematical Sciences, University of Cambridge, Wilberforce Road, Cambridge CB3 0WA, United Kingdom
(Received 14 January 2013; published 17 July 2013)

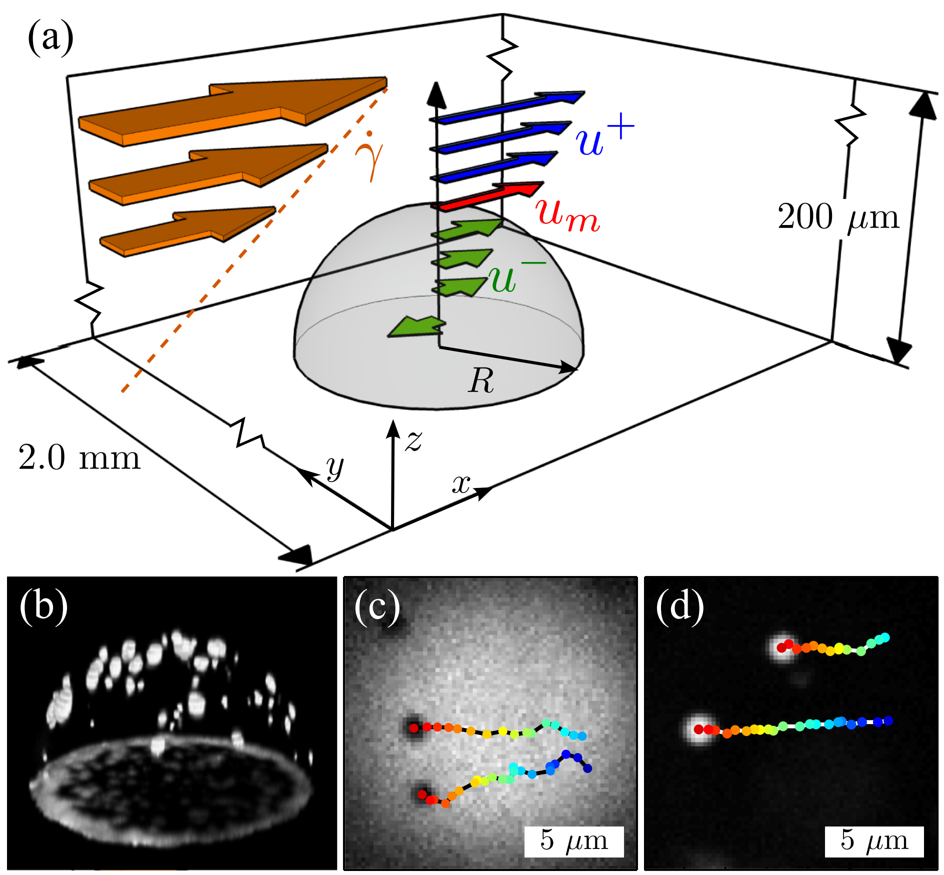

FIG. 1 (color online). Microfluidic shear experiment. (a) Schematic of the chamber (not to scale) and flows. (b) Confocal imaging reconstruction of an adhering hemispherical L_o phase vesicle with small L_d domains visible on its surface. (c)–(d) Tracking of gel domains in L_d background (c) and L_d domains in L_o background (d), flowing across the vesicle apex at $\dot{\gamma} = 2.6\ \mathrm{s}^{-1}$ (tracks color-coded in time over ~2.6 s).

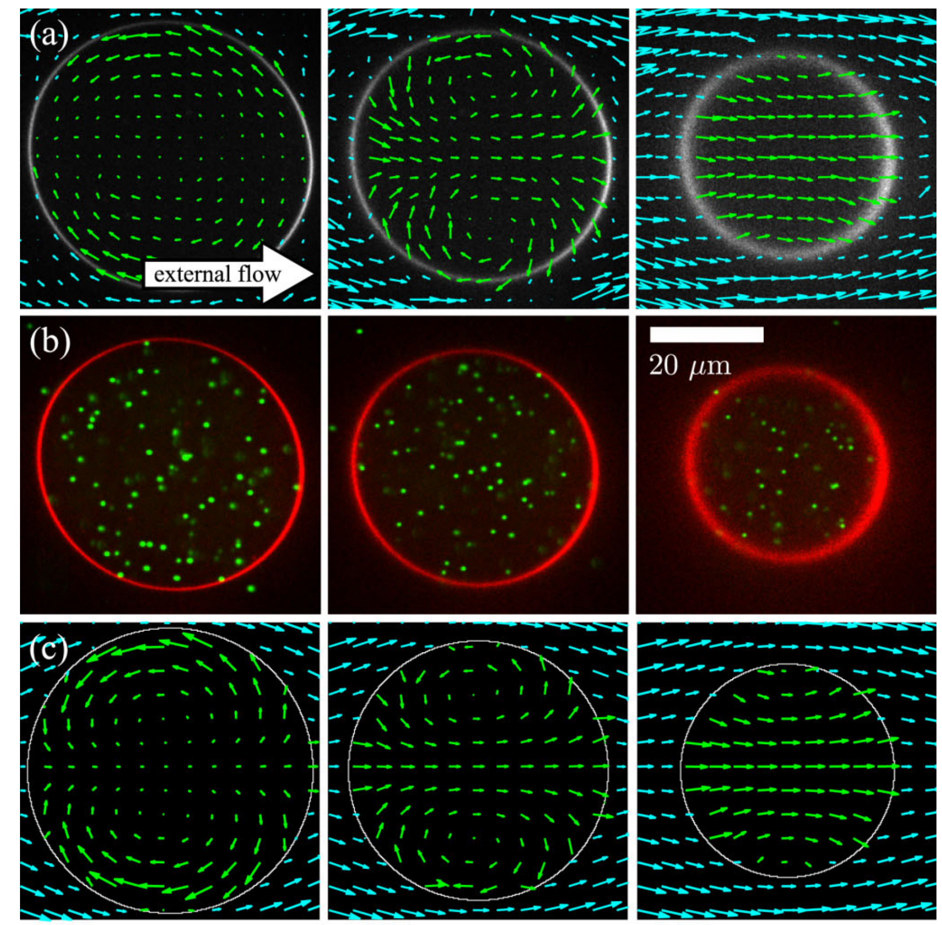

FIG. 2 (color online). Flow fields inside an adhering vesicle in shear. (a) Experimental two-dimensional PIV velocity fields at heights $z/R = 0.26$, 0.47, 0.71 above coverslip. (b) Confocal slices at same fractional heights as (a) show vesicle (red) containing fluorescent microspheres. (c) Theoretical two-dimensional velocity fields [25] for a sheared hemispherical vesicle at $z/R = 0.3$, 0.5, 0.7. Interior and exterior PIV vectors

Membrane Viscosity Determined from Shear-Driven Flow in Giant Vesicles

Aurelia R. Honerkamp-Smith, Francis G. Woodhouse, Vasily Kantsler, and Raymond E. Goldstein
Department of Applied Mathematics and Theoretical Physics, Centre for Mathematical Sciences, University of Cambridge, Wilberforce Road, Cambridge CB3 0WA, United Kingdom
(Received 14 January 2013; published 17 July 2013)

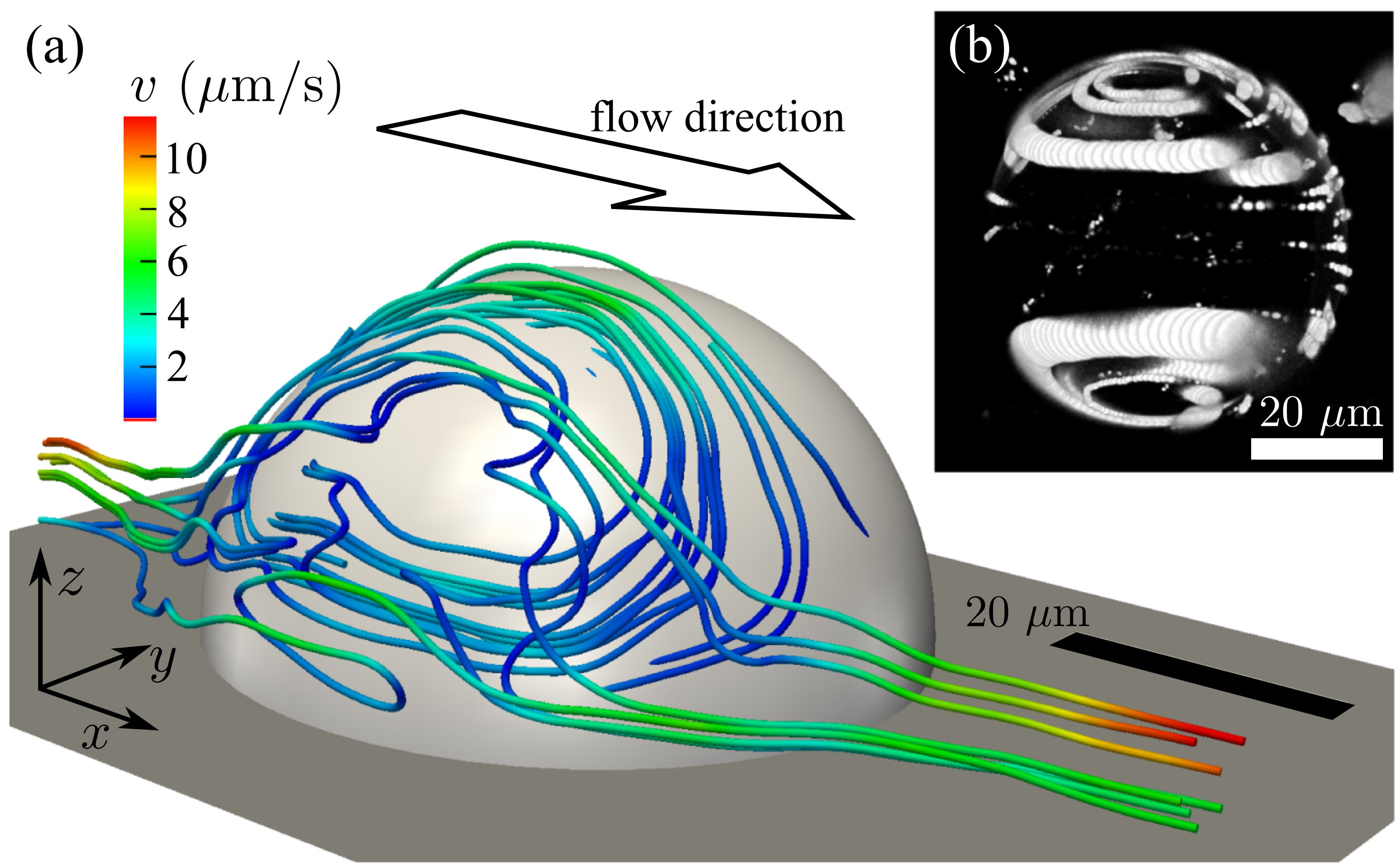

FIG. 3 (color online). Membrane and external flows. (a) Selected external streamlines along one side of an L_o vesicle in shear flow, showing closed orbits above the surface. (b) Time-lapse confocal stack of an L_o vesicle, viewed from above, illustrating circulation of L_d domains.

Membrane Viscosity Determined from Shear-Driven Flow in Giant Vesicles

Aurelia R. Honerkamp-Smith, Francis G. Woodhouse, Vasily Kantsler, and Raymond E. Goldstein
Department of Applied Mathematics and Theoretical Physics, Centre for Mathematical Sciences, University of Cambridge, Wilberforce Road, Cambridge CB3 0WA, United Kingdom
(Received 14 January 2013; published 17 July 2013)

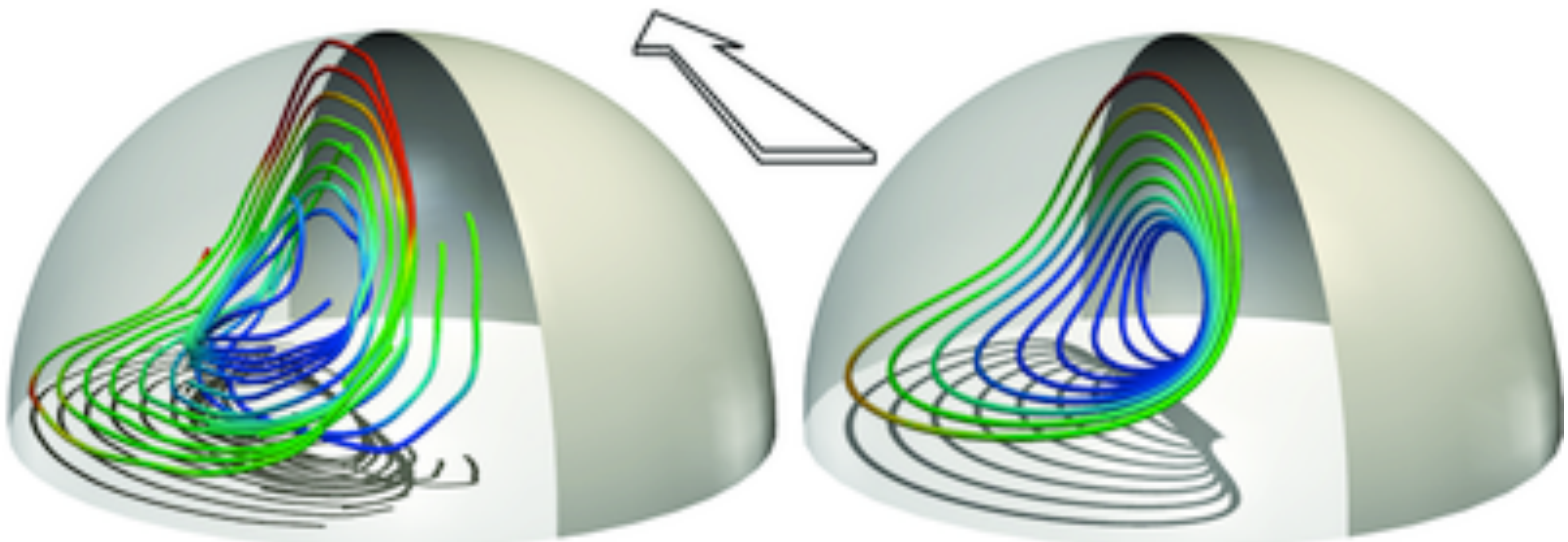

dunkel@math.mit.edu

PNAS

Dynamics of a vesicle in general flow

J. Deschamps, V. Kantsler, E. Segre, and V. Steinberg[1]

Department of Physics of Complex Systems, Weizmann Institute of Science, Rehovot, 76100 Israel

11444–11447 | PNAS | July 14, 2009 | vol. 106 | no. 28

APPLIE

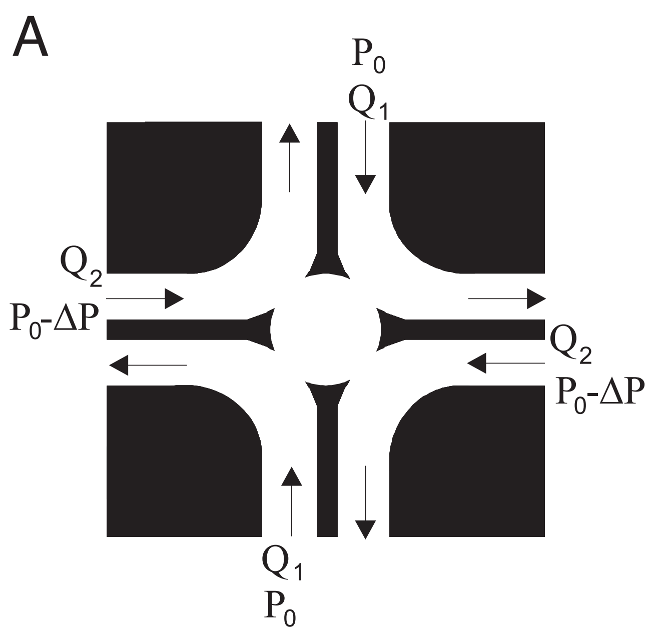

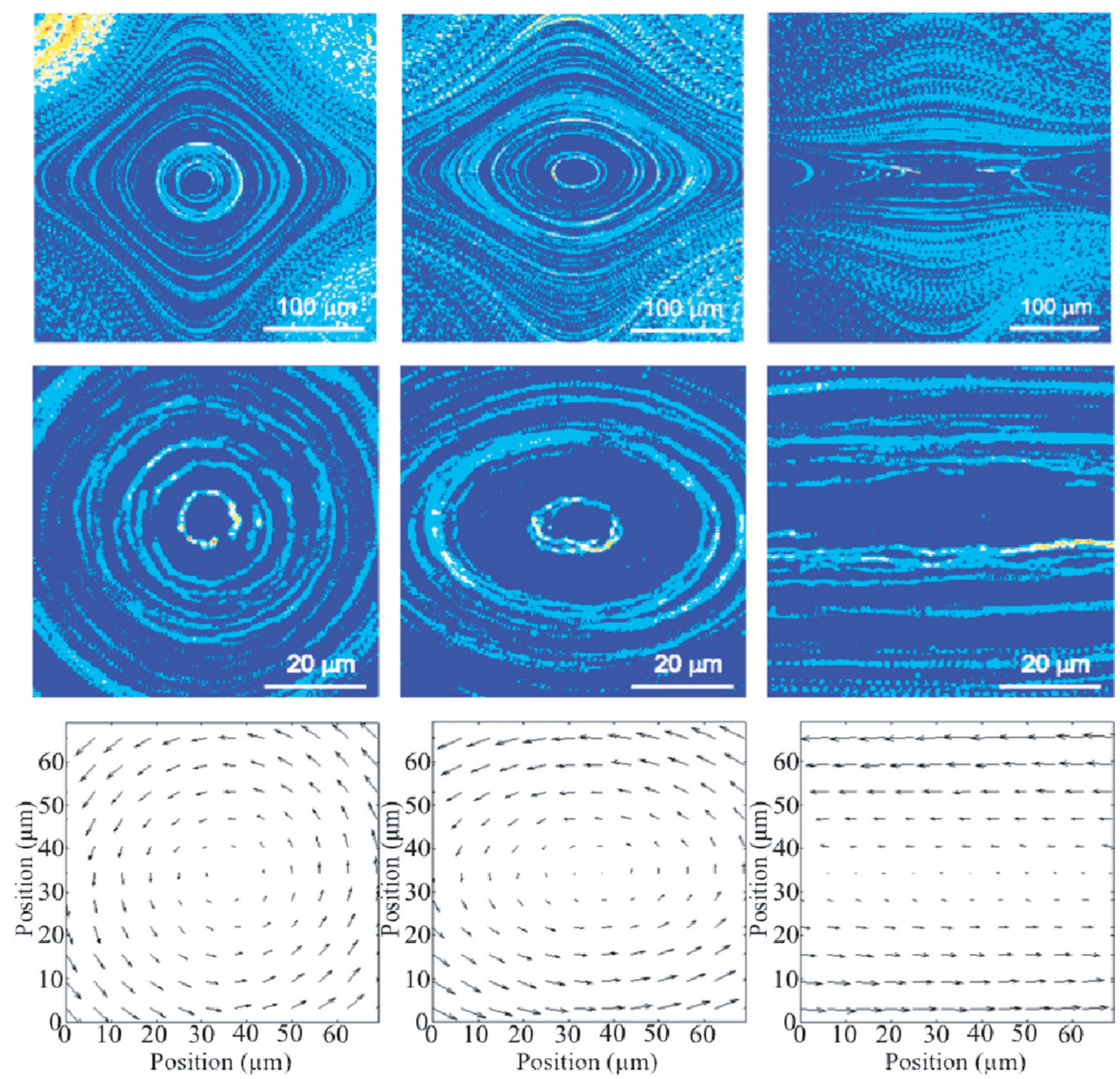

Fig. 2. (*A*) Experimental streamlines images of the velocity fields for pure rotational (first column, $\omega/s = 43$), mixed (second column, $\omega/s = 2.6$) and pure shear (third, $\omega/s = 1$) flows; (*B*) Zoom of the same experimental flows; (*C*) velocity vector field representation of the same flows (PTV).

dunkel@math.mit.edu

Dynamics of a vesicle in general flow

J. Deschamps, V. Kantsler, E. Segre, and V. Steinberg[1]

Department of Physics of Complex Systems, Weizmann Institute of Science, Rehovot, 76100 Israel

11444–11447 | PNAS | July 14, 2009 | vol. 106 | no. 28

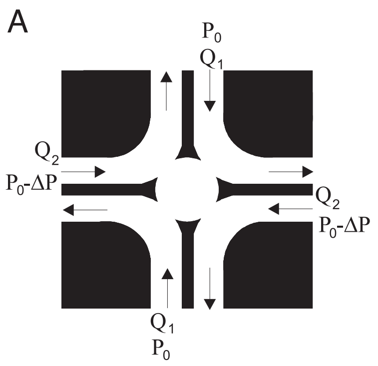

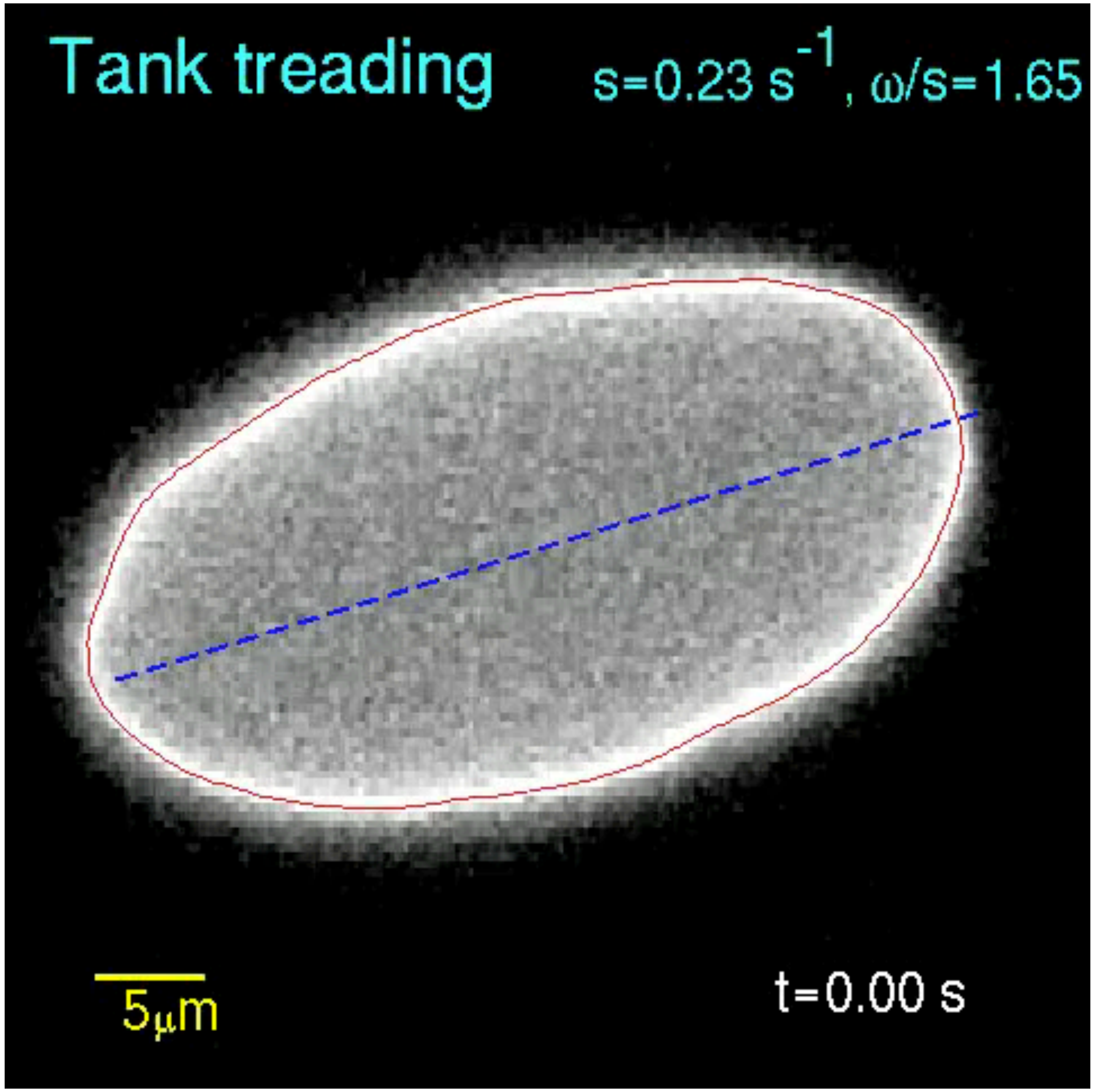

dunkel@math.mit.edu

NATURE | VOL 423 | 8 MAY 2003 | www.nature.com/nature

Controlled vesicle deformation and lysis by single oscillating bubbles

Philippe Marmottant & Sascha Hilgenfeldt

Faculty of Applied Physics, University of Twente, PO Box 217, 7500AE Enschede, The Netherlands

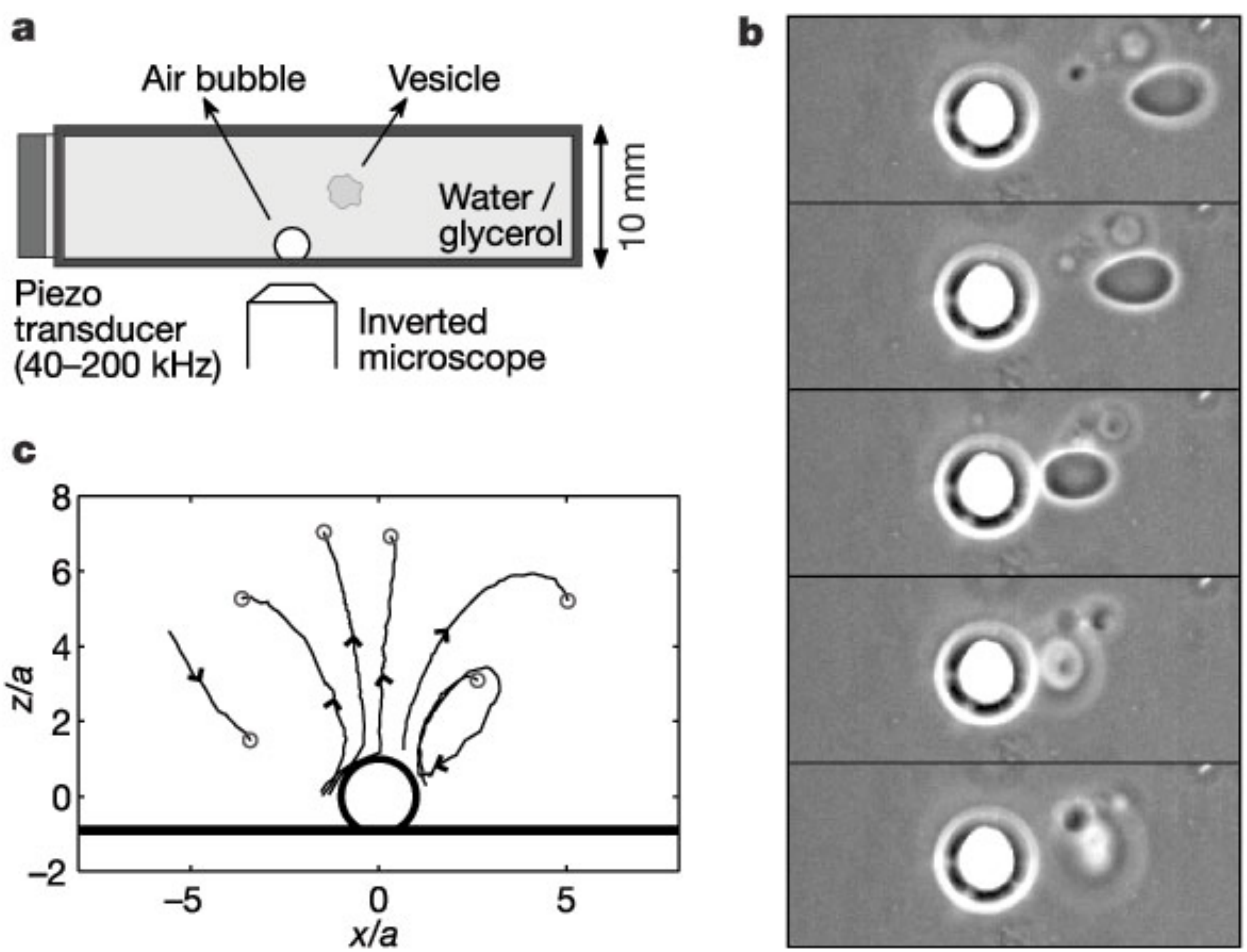

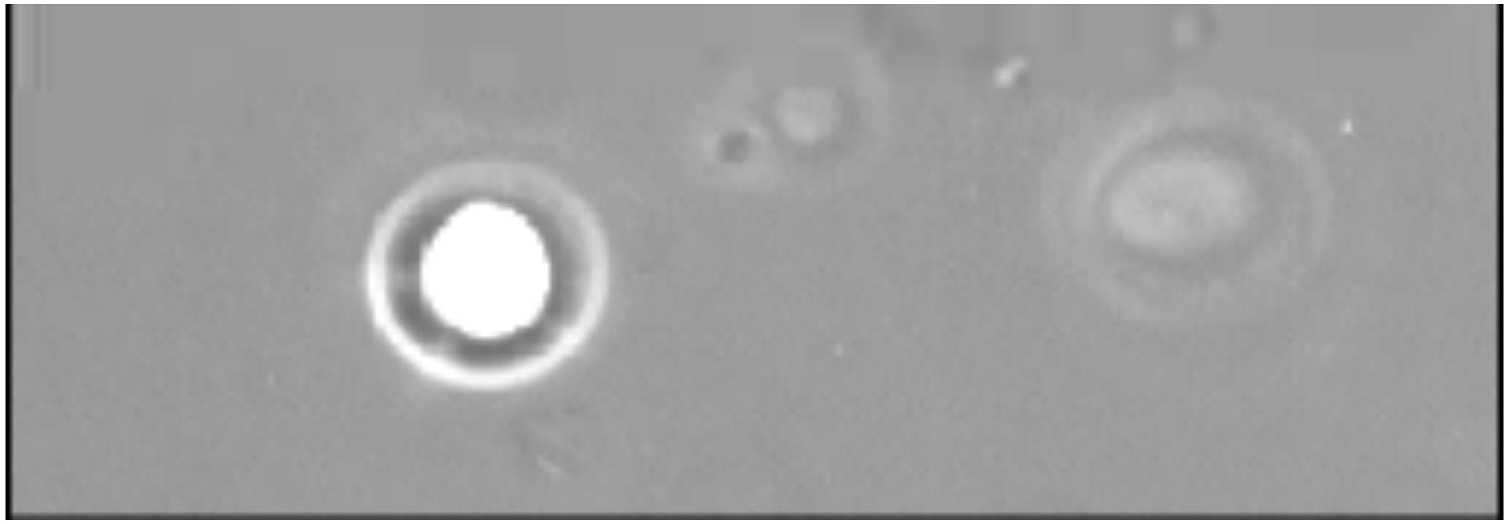

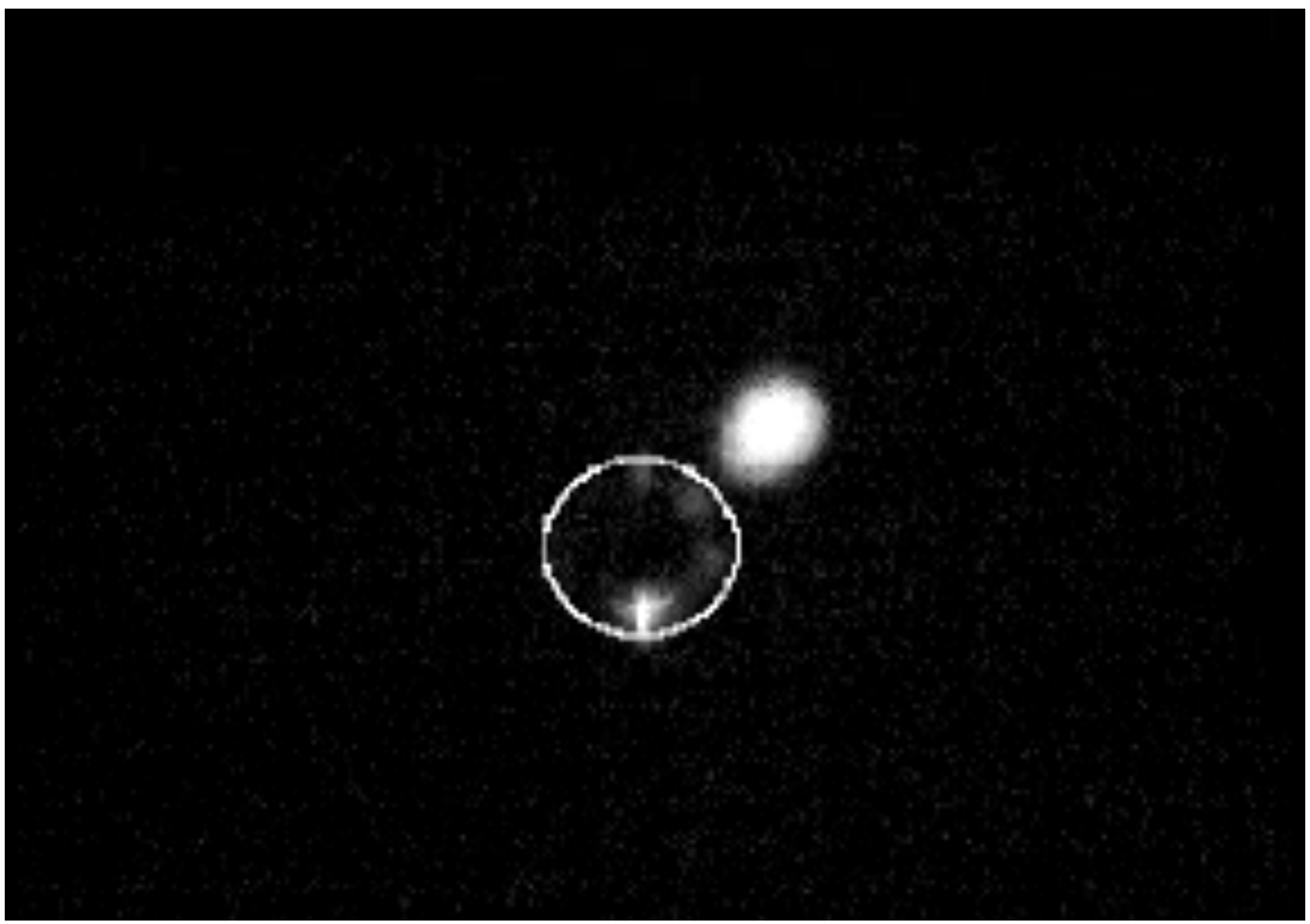

NATURE | VOL 423 | 8 MAY 2003 | www.nature.com/nature

letters to nature

Controlled vesicle deformation and lysis by single oscillating bubbles

Philippe Marmottant & Sascha Hilgenfeldt

Faculty of Applied Physics, University of Twente, PO Box 217, 7500AE Enschede, The Netherlands

dunkel@math.mit.edu

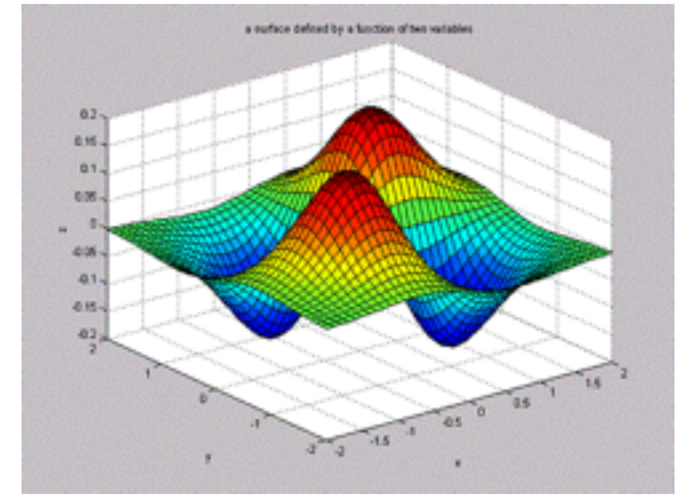

Membranes

The discussion in this section builds on the review article [Sei97] and the textbook [OLXY99].

Reminder: 2D differential geometry

We consider an orientable surface in $\mathbb{R}^3$. Possible local parameterizations are

$$\boldsymbol{F}(s_1, s_2) \in \mathbb{R}^3 \tag{3.1}$$

where $(s_1, s_2) \in U \subseteq \mathbb{R}^2$. Alternatively, if one chooses Cartesian coordinates $(s_1, s_2) = (x, y)$, then it suffices to specify

$$z = f(x, y) \tag{3.2a}$$

or, equivalently, the implicit representation

$$\Phi(x, y, z) = z - f(x, y). \tag{3.2b}$$

The vector representation (3.1) can be related to the 'height' representation (3.2a) by

$$\boldsymbol{F}(x, y) = \begin{pmatrix} x \\ y \\ f(x, y) \end{pmatrix} \tag{3.3}$$

Surface metric tensor

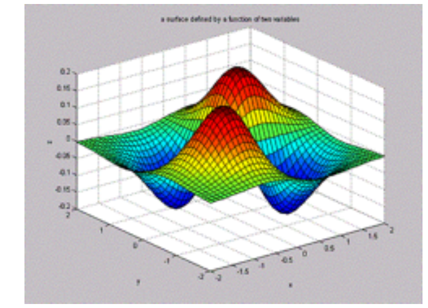

$$\boldsymbol{F}(x,y) = \begin{pmatrix} x \\ y \\ f(x,y) \end{pmatrix} \tag{3.3}$$

Denoting derivatives by $\boldsymbol{F}_i = \partial_{s_i}\boldsymbol{F}$, we introduce the surface metric tensor $g = (g_{ij})$ by

$$g_{ij} = \boldsymbol{F}_i \cdot \boldsymbol{F}_j, \tag{3.4a}$$

abbreviate its determinant by

$$|g| := \det g, \tag{3.4b}$$

and define the associated Laplace-Beltrami operator ∇^2 by

$$\nabla^2 h = \frac{1}{\sqrt{|g|}}\partial_i(g_{ij}^{-1}\sqrt{|g|}\partial_j h), \tag{3.4c}$$

for some function $h(s_1, s_2)$.

dunkel@math.mit.edu

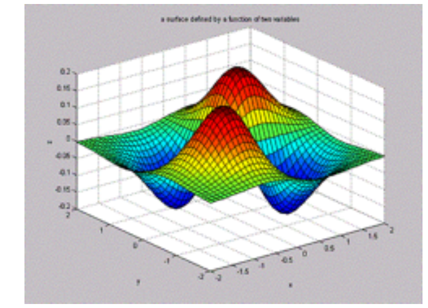

$$\boldsymbol{F}(x,y) = \begin{pmatrix} x \\ y \\ f(x,y) \end{pmatrix} \tag{3.3}$$

Denoting derivatives by $\boldsymbol{F}_i = \partial_{s_i}\boldsymbol{F}$, we introduce the surface metric tensor $g = (g_{ij})$ by

$$g_{ij} = \boldsymbol{F}_i \cdot \boldsymbol{F}_j, \tag{3.4a}$$

abbreviate its determinant by

$$|g| := \det g, \tag{3.4b}$$

$$\boldsymbol{F}_x(x,y) = \begin{pmatrix} 1 \\ 0 \\ f_x \end{pmatrix}, \qquad \boldsymbol{F}_y(x,y) = \begin{pmatrix} 0 \\ 1 \\ f_y \end{pmatrix} \tag{3.5}$$

and, hence, the metric tensor

$$g = (g_{ij}) = \begin{pmatrix} \boldsymbol{F}_x \cdot \boldsymbol{F}_x & \boldsymbol{F}_x \cdot \boldsymbol{F}_y \\ \boldsymbol{F}_y \cdot \boldsymbol{F}_x & \boldsymbol{F}_y \cdot \boldsymbol{F}_y \end{pmatrix} = \begin{pmatrix} 1+f_x^2 & f_x f_y \\ f_y f_x & 1+f_y^2 \end{pmatrix} \tag{3.6a}$$

and its determinant

$$|g| = 1 + f_x^2 + f_y^2, \tag{3.6b}$$

where $f_x = \partial_x f$ and $f_y = \partial_y f$. For later use, we still note that the inverse of the metric tensor is given by

$$g^{-1} = (g_{ij}^{-1}) = \frac{1}{1+f_x^2+f_y^2} \begin{pmatrix} 1+f_y^2 & -f_x f_y \\ -f_y f_x & 1+f_x^2 \end{pmatrix}. \tag{3.6c}$$

dunkel@math.mit.edu

Surface normal & curvature

Assuming the surface is regular at (s_1, s_2), which just means that the tangent vectors $\boldsymbol{F}_1$ and $\boldsymbol{F}_2$ are linearly independent, the local unit normal vector is defined by

$$\boldsymbol{N} = \frac{\boldsymbol{F}_1 \wedge \boldsymbol{F}_2}{||\boldsymbol{F}_1 \wedge \boldsymbol{F}_2||}. \tag{3.7}$$

In terms of the Cartesian parameterization, this can also be rewritten as

$$\boldsymbol{N} = \frac{\nabla\Phi}{||\nabla\Phi||} = \frac{1}{\sqrt{1 + f_x^2 + f_y^2}} \begin{pmatrix} -f_x \\ -f_y \\ 1 \end{pmatrix}. \tag{3.8}$$

Here, we have adopted the convention that $\{\boldsymbol{F}_1, \boldsymbol{F}_2, \boldsymbol{N}\}$ form a right-handed system.

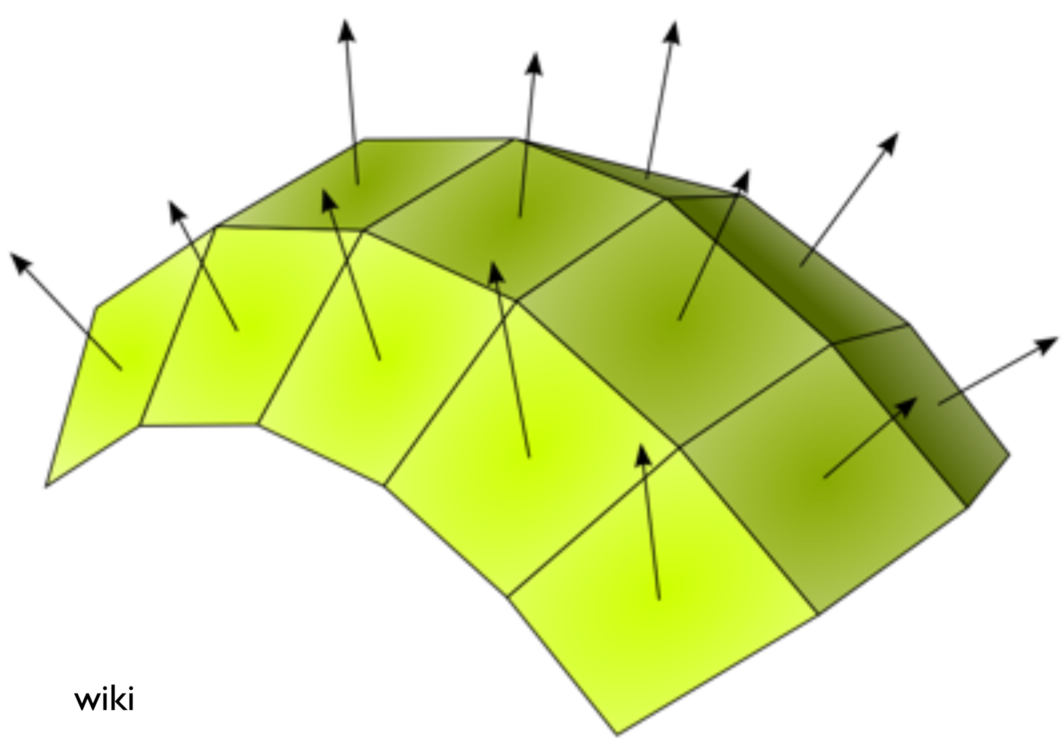

wiki

dunkel@math.mit.edu

Surface normal & curvature

Assuming the surface is regular at (s_1, s_2), which just means that the tangent vectors $\boldsymbol{F}_1$ and $\boldsymbol{F}_2$ are linearly independent, the local unit normal vector is defined by

$$\boldsymbol{N} = \frac{\boldsymbol{F}_1 \wedge \boldsymbol{F}_2}{||\boldsymbol{F}_1 \wedge \boldsymbol{F}_2||}. \tag{3.7}$$

In terms of the Cartesian parameterization, this can also be rewritten as

$$\boldsymbol{N} = \frac{\nabla\Phi}{||\nabla\Phi||} = \frac{1}{\sqrt{1 + f_x^2 + f_y^2}} \begin{pmatrix} -f_x \\ -f_y \\ 1 \end{pmatrix}. \tag{3.8}$$

Here, we have adopted the convention that $\{\boldsymbol{F}_1, \boldsymbol{F}_2, \boldsymbol{N}\}$ form a right-handed system.

To formulate 'geometric' energy functionals for membranes, we still require the concept of curvature, which quantifies the local bending of the membrane. We define a 2×2-curvature tensor $R = (R_{ij})$ by

$$R_{ij} = \boldsymbol{N} \cdot (\boldsymbol{F}_{ij}) \tag{3.9}$$

and local *mean curvature* H and local *Gauss curvature* K by

$$H = \frac{1}{2}\mathrm{tr}\,(g^{-1} \cdot R)\;, \qquad K = \det(g^{-1} \cdot R). \tag{3.10}$$

Adopting the Cartesian representation (3.2a), we have

$$\boldsymbol{F}_{xx} = \begin{pmatrix} 0 \\ 0 \\ f_{xx} \end{pmatrix}\;, \qquad \boldsymbol{F}_{xy} = \boldsymbol{F}_{yx} = \begin{pmatrix} 0 \\ 0 \\ f_{xy} \end{pmatrix}\;, \qquad \boldsymbol{F}_{yy} = \begin{pmatrix} 0 \\ 0 \\ f_{yy} \end{pmatrix} \tag{3.11a}$$

Surface normal & curvature

yielding the curvature tensor

$$(R_{ij}) = \begin{pmatrix} \boldsymbol{N} \cdot \boldsymbol{F}_{xx} & \boldsymbol{N} \cdot \boldsymbol{F}_{xy} \\ \boldsymbol{N} \cdot \boldsymbol{F}_{yx} & \boldsymbol{N} \cdot \boldsymbol{F}_{yy} \end{pmatrix} = \frac{1}{\sqrt{1 + f_x^2 + f_y^2}} \begin{pmatrix} f_{xx} & f_{xy} \\ f_{yx} & f_{yy} \end{pmatrix} \tag{3.11b}$$

Denoting the eigenvalues of the matrix $g^{-1} \cdot R$ by κ_1 and κ_2, we obtain for the mean curvature

$$H = \frac{1}{2}(\kappa_1 + \kappa_2) = \frac{(1 + f_y^2) f_{xx} - 2 f_x f_y f_{xy} + (1 + f_x^2) f_{yy}}{2(1 + f_x^2 + f_y^2)^{3/2}} \tag{3.12}$$

and for the Gauss curvature

$$K = \kappa_1 \cdot \kappa_2 = \frac{f_{xx} f_{yy} - f_{xy}^2}{(1 + f_x^2 + f_y^2)^2}. \tag{3.13}$$

dunkel@math.mit.edu

Gauss-Bonet Theorem

$$\int_M K \, dA + \oint_{\partial M} k_g \, ds = 2\pi \, \chi(M). \tag{3.14}$$

Gauss curvature | geodesic curvature | Euler characteristic

$\chi(M) = 2 - 2g$, where g is the *genus*

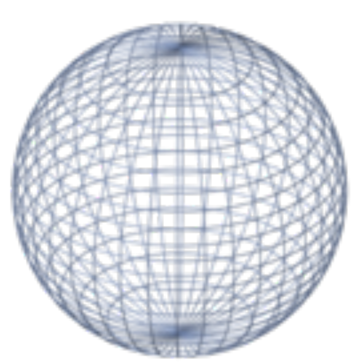

2

0

-2

wiki

dunkel@math.mit.edu

Gauss-Bonet Theorem

$$\int_M K\,dA + \oint_{\partial M} k_g\,ds = 2\pi\,\chi(M). \tag{3.14}$$

Convex polyhedra

Name	Image	Vertices *V*	Edges *E*	Faces *F*	Euler characteristic: *V* − *E* + *F*
Tetrahedron		4	6	4	**2**
Hexahedron or cube	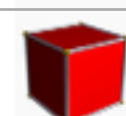	8	12	6	**2**
Octahedron		6	12	8	**2**
Dodecahedron		20	30	12	**2**
Icosahedron		12	30	20	**2**

wiki

Minimal surfaces

Minimal surfaces are surfaces that minimize the area within a given contour ∂M,

$$A(M|\partial M) = \int_M dA = \min! \tag{3.15}$$

Assuming a Cartesian parameterization $z = f(x, y)$ and abbreviating $f_i = \partial_i f$ as before, we have

$$dA = \sqrt{|g|}\, dxdy = \sqrt{1 + f_x^2 + f_y^2}\, dxdy =: \mathcal{L}\, dxdy, \tag{3.16}$$

catenoid

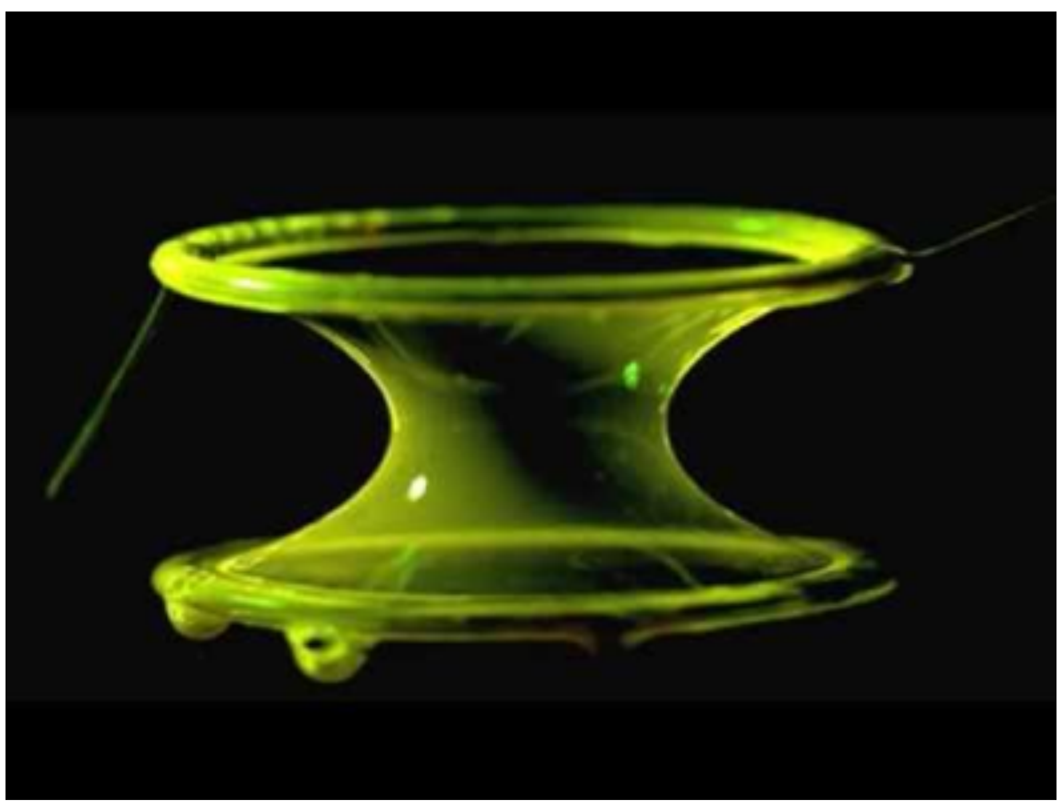

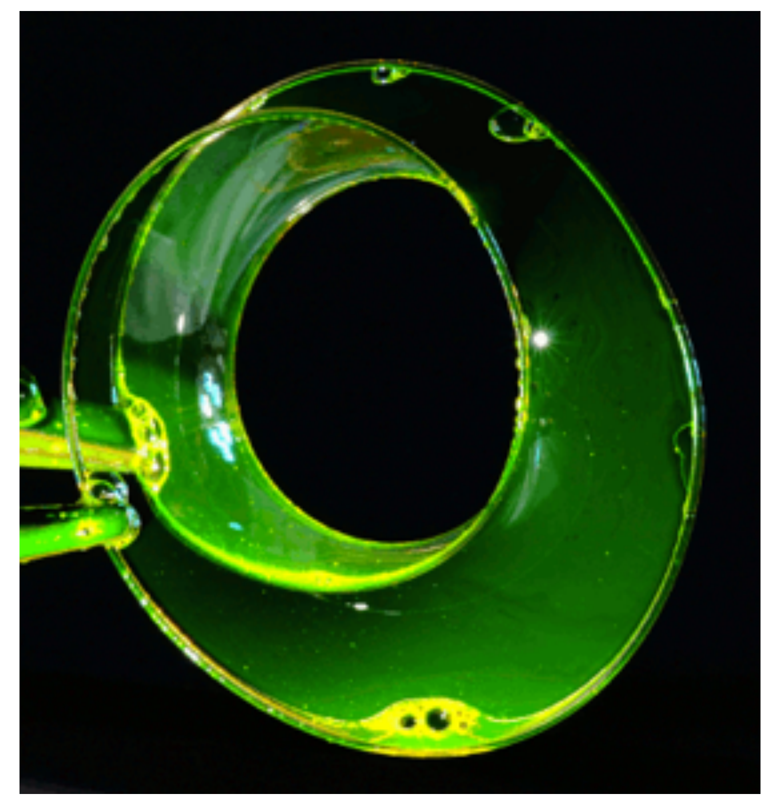

Goldstein lab (Cambridge)

dunkel@math.mit.edu

Minimal surfaces

Minimal surfaces are surfaces that minimize the area within a given contour ∂M,

$$A(M|\partial M) = \int_M dA = \text{min!} \tag{3.15}$$

Assuming a Cartesian parameterization $z = f(x,y)$ and abbreviating $f_i = \partial_i f$ as before, we have

$$dA = \sqrt{|g|}\, dxdy = \sqrt{1 + f_x^2 + f_y^2}\, dxdy =: \mathcal{L}\, dxdy, \tag{3.16}$$

and the minimum condition (3.15) can be expressed in terms of the Euler-Lagrange equations

$$0 = \frac{\delta A}{\delta f} = -\partial_i \frac{\partial \mathcal{L}}{\partial f_i}. \tag{3.17}$$

Inserting the Lagrangian $\mathcal{L} = \sqrt{|g|}$, one finds

$$0 = -\left[\partial_x \left(\frac{f_x}{\sqrt{1 + f_x^2 + f_y^2}}\right) + \partial_y \left(\frac{f_y}{\sqrt{1 + f_x^2 + f_y^2}}\right)\right] \tag{3.18}$$

which may be recast in the form

$$0 = \frac{(1 + f_y^2) f_{xx} - 2 f_x f_y f_{xy} + (1 + f_x^2) f_{yy}}{(1 + f_x^2 + f_y^2)^{3/2}} = -2H. \tag{3.19}$$

dunkel@math.mit.edu

Minimal surfaces

Minimal surfaces are surfaces that minimize the area within a given contour ∂M,

$$A(M|\partial M) = \int_M dA = \text{min!} \tag{3.15}$$

Assuming a Cartesian parameterization $z = f(x, y)$ and abbreviating $f_i = \partial_i f$ as before, we have

$$dA = \sqrt{|g|}\, dxdy = \sqrt{1 + f_x^2 + f_y^2}\, dxdy =: \mathcal{L}\, dxdy, \tag{3.16}$$

and the minimum condition (3.15) can be expressed in terms of the Euler-Lagrange equations

$$0 = \frac{\delta A}{\delta f} = -\partial_i \frac{\partial \mathcal{L}}{\partial f_i}. \tag{3.17}$$

Thus, minimal surfaces satisfy

$$H = 0 \qquad \Leftrightarrow \qquad \kappa_1 = -\kappa_2, \tag{3.20}$$

implying that each point of a minimal surface is a saddle point.

dunkel@math.mit.edu

Helfrich's model

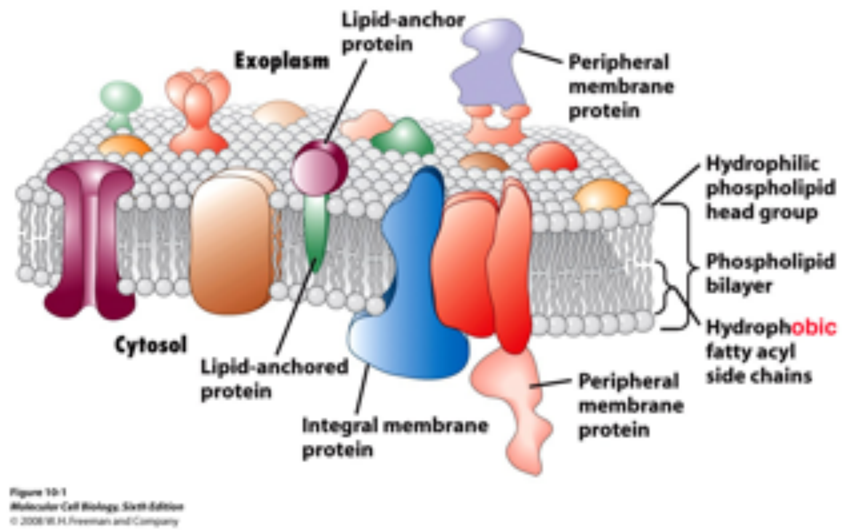

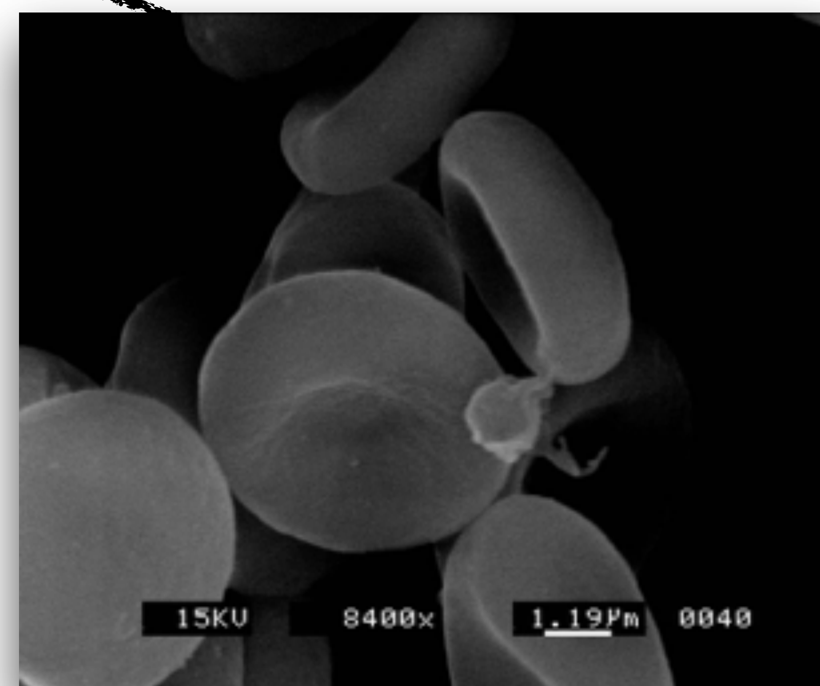

wiki

www.math.tamu.edu/~bonito/

Helfrich's model

Assuming that lipid bilayer membranes can be viewed as two-dimensional surfaces, Helfrich [Hel73] proposed in 1973 the following geometric curvature energy per unit area for a closed membrane

$$f_c = \frac{k_c}{2}(2H - c_0)^2 + k_G\, K, \tag{3.31}$$

where constants k_c, k_G are bending rigidities and c_0 is the spontaneous curvature of the membrane. The full free energy for a closed membrane can then be written as

$$F_c = \int dA\; f_c + \sigma \int dA + \Delta p \int dV, \tag{3.32}$$

where σ is the surface tension and Δp the osmotic pressure (outer pressure minus inner pressure). Minimizing F with respect to the surface shape, one finds after some heroic manipulations the shape equation[2]

$$\Delta p - 2\sigma H + k_c(2H - c_0)(2H^2 + c_0 H - 2K) + k_c \nabla^2 (2H - c_0) = 0, \tag{3.33}$$

where ∇^2 is the Laplace-Beltrami operator on the surface. The derivation of Eq. (3.33) uses our earlier result

$$\frac{\delta A}{\delta f} = -2H, \tag{3.34}$$

and the fact that the volume integral may be rewritten as[3]

$$V = \int dV = \int dA\; \frac{1}{3} \boldsymbol{F} \cdot \boldsymbol{N}\;, \tag{3.35}$$

$dV = \frac{1}{3} h\, dA$ for a cone or pyramid of height $h = \boldsymbol{F} \cdot \boldsymbol{N}$

dunkel@math.mit.edu

Helfrich's model

Assuming that lipid bilayer membranes can be viewed as two-dimensional surfaces, Helfrich [Hel73] proposed in 1973 the following geometric curvature energy per unit area for a closed membrane

$$f_c = \frac{k_c}{2}(2H - c_0)^2 + k_G\, K, \tag{3.31}$$

where constants k_c, k_G are bending rigidities and c_0 is the spontaneous curvature of the membrane. The full free energy for a closed membrane can then be written as

$$F_c = \int dA\; f_c + \sigma \int dA + \Delta p \int dV, \tag{3.32}$$

where σ is the surface tension and Δp the osmotic pressure (outer pressure minus inner pressure). Minimizing F with respect to the surface shape, one finds after some heroic manipulations the shape equation[2]

$$\Delta p - 2\sigma H + k_c(2H - c_0)(2H^2 + c_0 H - 2K) + k_c \nabla^2(2H - c_0) = 0, \tag{3.33}$$

where ∇^2 is the Laplace-Beltrami operator on the surface. The derivation of Eq. (3.33) uses our earlier result

$$\frac{\delta A}{\delta f} = -2H, \tag{3.34}$$

and the fact that the volume integral may be rewritten as[3]

$$V = \int dV = \int dA\; \frac{1}{3}\boldsymbol{F} \cdot \boldsymbol{N}\ , \tag{3.35}$$

$$\Rightarrow \quad \frac{\delta V}{\delta f} = 1.$$

dunkel@math.mit.edu

Helfrich's model

Assuming that lipid bilayer membranes can be viewed as two-dimensional surfaces, Helfrich [Hel73] proposed in 1973 the following geometric curvature energy per unit area for a closed membrane

$$f_c = \frac{k_c}{2}(2H - c_0)^2 + k_G\, K, \tag{3.31}$$

where constants k_c, k_G are bending rigidities and c_0 is the spontaneous curvature of the membrane. The full free energy for a closed membrane can then be written as

$$F_c = \int dA\, f_c + \sigma \int dA + \Delta p \int dV, \tag{3.32}$$

where σ is the surface tension and Δp the osmotic pressure (outer pressure minus inner pressure). Minimizing F with respect to the surface shape, one finds after some heroic manipulations the shape equation[2]

$$\Delta p - 2\sigma H + k_c(2H - c_0)(2H^2 + c_0 H - 2K) + k_c \nabla^2 (2H - c_0) = 0, \tag{3.33}$$

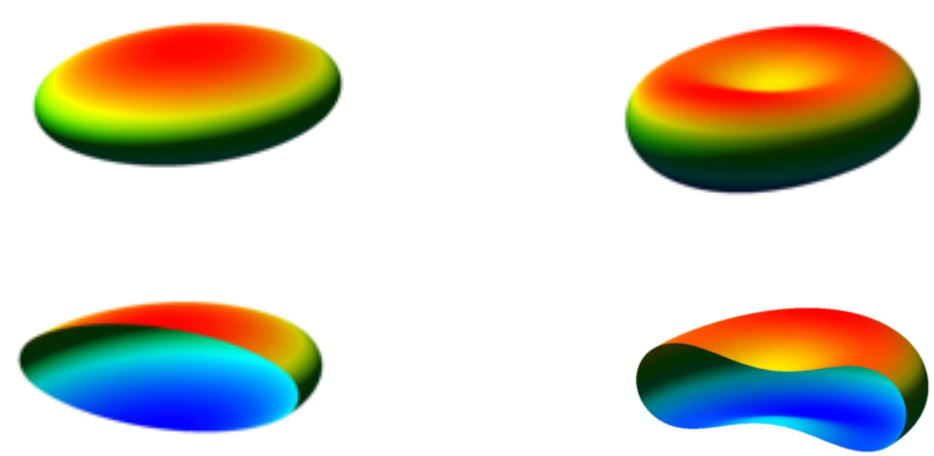

www.math.tamu.edu/~bonito/

dunkel@math.mit.edu

Helfrich's model

Assuming that lipid bilayer membranes can be viewed as two-dimensional surfaces, Helfrich [Hel73] proposed in 1973 the following geometric curvature energy per unit area for a closed membrane

$$f_c = \frac{k_c}{2}(2H - c_0)^2 + k_G K, \tag{3.31}$$

where constants k_c, k_G are bending rigidities and c_0 is the spontaneous curvature of the membrane. The full free energy for a closed membrane can then be written as

$$F_c = \int dA\, f_c + \sigma \int dA + \Delta p \int dV, \tag{3.32}$$

For open membranes with boundary ∂M, a plausible energy functional is given by

$$F_o = \int dA\, f_c + \sigma \int dA + \gamma \oint_{\partial M} ds, \tag{3.37}$$

where γ is the line tension of the boundary. In this case, variation yields not only the corresponding shape equation but also a non-trivial set of boundary conditions.

dunkel@math.mit.edu